A new Late Cretaceous to Present APWP for Asia and its implications for paleomagnetic shallow inclinations in Central Asia and Cenozoic Eurasian plate deformation

Jean-Pascal Cogné, Jean Besse, Yan Chen, Fatim Hankard

A new Late Cretaceous to Present APWP for Asia and its bearing upon shallow inclinations issue in Asia and Eurasia plate deformation.

Jean-Pascal Cogné[1*], Jean Besse[1], Yan Chen[2], Fatim Hankard[1]

[1] *Equipe de Paléomagnétisme, Institut de Physique du Globe, Sorbonne Paris Cité, Université Paris Diderot, CNRS UMR 7154, F-75005 Paris, France;*

[2] *Université d'Orléans, UMR 6113 CNRS, 1A rue de la Férollerie, 45000 Orléans, France;*

[*] Corresponding author*; e-mail:* cogne@ipgp.fr

Short title: East Asia APWP and Eurasia deformation

Abstract.

Based on a compilation of 533 Cretaceous to present-day paleomagnetic poles obtained from both sedimentary and igneous rocks, we present a new analysis of the so-called "Asian inclination anomaly" and demonstrated the anomaly to be twofold: a 2nd-order anomaly, characterized by high paleolatitudes in Indochina and low paleolatitudes over Tibet and Central Asia, is superimposed on a 1st-order anomaly, characterized by Cenozoic low paleolatitudes found all over north-eastern Asian stable blocks. The analysis herein convincingly shows that the Europe Apparent Polar Wandering Path (APWP) can no longer be used to interpret paleomagnetic data East of the Urals, including interpretation of Asian Tertiary deformation related to the India-Asia Collision. We thus construct a new APWP for East Asia, based on paleopoles from blocks assumed to be stable. This new APWP is consistent with and reinforces previous analyses of Asian tectonics, such as the age (~55 Ma) and locus (~5-10° N) of the Indo-Asian collision, the lateral extrusion of SE Asian continental blocks, and the intracontinental shortening in Central Asia. Possible origins of the 1st-order paleolatitude anomaly are: (1) a geomagnetic origin, due to long-lasting non-dipolar contribution to the magnetic field, and (2) a tectonic hypothesis, in which a newly defined East Asia plate was located ~10° farther south than expected from the current Europe APWP. Based on a set of 6 new reconstructions from 90 Ma to Present, we show that our tectonic model reconciles geophysical, geological and tectonic observations throughout Eurasia, from Siberia to Europe, including kinematics in the Arctic Ocean, up to northwestern Arctic Alaska. Beyond possible occurrences of non-dipolar field contribution and/or local inclination flattening in the sedimentary data, our model leads us to conclude that Cenozoic tectonics is the dominant contributor to the observed 1st-order ~10° low paleolatitude anomaly over Asia during the Tertiary.

1. Introduction.

After some decades of paleomagnetic research conducted on Meso-Cenozoic rock formations of Asia, a long-lasting and puzzling problem is still now not satisfactorily deciphered, the so-called Inclination, or Paleolatitude Anomaly. In fact, a large amount of paleomagnetic results coming from widely distributed localities over Asia, with primary magnetization, often exhibit inclinations significantly lower than expected from the Meso-Cenozoic part of the assumed reference Apparent Polar Wandering Path (APWP) for Eurasia (e.g. Westphal, 1993; Thomas et al., 1994; Chauvin et al., 1996; Halim et al., 1998a; Cogné et al., 1999; Hankard et al., 2007a, and references therein). The most widely used reference APWP for analysing Asian paleomagnetic results has usually been the Europe APWP of Besse and Courtillot (1991), reappraised by Besse and Courtillot (2002). We remind the reader that this APWP has been constructed by calculating a synthetic APWP on a fixed continent, Africa, after transferring worldwide paleomagnetic data onto it, using plate circuits defined by ocean floor isochrons and resulting rotation parameters (e.g. Müller et al. 1997, 2008), and then re-transferring the calculated master synthetic APWP onto each continent. A crucial point is that Europe APWP can only serve as a reference for comparison with experimentally determined paleopoles of Asia if, and only if, whole Eurasia was indeed constituted and behaving as a single rigid plate at least since the Mesozoic. We demonstrate in this paper that this is a critical point in the analysis of low paleolatitude anomaly.

Cretaceous Paleomagnetic results from northeastern Asian regions (Fig. 1), Siberia and Amuria (e.g. Enkin et al., 1992; Pruner, 1992; Chen et al., 1993b; Halim et al., 1998a, b; Cogné et al., 2005; Hankard et al., 2007b; van Hinsbergen et al., 2008), North and South China blocks (NCB and SCB; e.g. Lin et al. 1985; Zhao and Coe 1987; Huang & Opdyke 1991; Enkin et al. 1991, 1992; Yang et al. 1992; Gilder et al. 1993a, 1996; Gilder & Courtillot 1997; Yang and Besse, 2003) often show local rotations around vertical axes, but do not significantly depart from Besse and Courtillot (1991, 2002) Europe APWP in terms of expected paleolatitude. This lends support to the ideas that (1) these blocks or terranes form a stable area since the Cretaceous, (2) Eurasia indeed forms a single rigid plate since that time and thus (3) the Europe APWP could serve as a reference to describe any discrepancies that could be observed in other Asian regions. As a matter of fact, widely observed Cretaceous shallow paleomagnetic inclinations from Tibetan and central Asian blocks (e.g. Achache et al., 1984; Besse et al., 1984; Chen et al, 1992, 1993a, 1993b; Halim et al., 1998a; Cogné et al., 1995) have been interpreted as resulting from sites paleolatitudes which were farther south than expected. Subsequently, these mobile blocks were supposed to have drifted northward

with respect to stable Siberia, and undergone relative intracontinental shortening between India and Siberia due to the ongoing penetration of the India plate into Eurasia, after its collision at ~50 Ma. Similarly, Mesozoic paleomagnetic inclinations from Northern Thailand (e.g. Yang and Besse, 1993), were found steeper than expected from the Eurasia APWP, and interpreted as resulting from southeastward extrusion of the Indochina Peninsula. The amount of convergence and the distribution of shortening between the various blocks (e.g., Chen et al., 1993b), together with lateral extrusion of blocks, revealed to be consistent with tectonic deformation models for Asia under the effect of a northward convergence of India with Siberia (e.g., Molnar and Tapponnier, 1975; Tapponnier and Molnar, 1979; Tapponnier et al., 1982; Replumaz and Tapponnier, 2003).

However, paleomagnetic data obtained on Tertiary formations from Central Asia are unexpectedly inconsistent with this picture. Tertiary paleomagnetic inclinations from Central Asia are, as for the Cretaceous, shallower than those predicted from the Europe APWP, but the amount of northward drift of blocks and intracontinental shortening deduced from these shallow inclinations are apparently at least twice as large as the amount deduced from the Cretaceous data. First described by Westphal (1993), these anomalously shallow magnetizations have been described all over Central Asia and Tibet (e.g. Thomas et al., 1994; Chauvin et al., 1996; Cogné et al., 1999; Dupont-Nivet et al., 2002, 2010b; Gilder et al., 2003; Tan et al., 2003, 2010, amongst other). More puzzling, recent studies of Hankard et al. (2007a) have demonstrated the presence of this anomaly in basalts from Mongolia, in the Amuria block, which is supposed to be part of the "stable" part of Asia, after its amalgamation to Siberia at the end of the Jurassic (Kravchinsky et al., 2002; Cogné et al., 2005, Metelkin et al., 2007, 2010; Kovalenko, 2010).

As proposed by Cogné et al. (1999), three main causes may be considered as responsible for this anomaly and have been recently debated in the literature: (1) a flattening of paleomagnetic inclination due to some sedimentary processes such as compaction and/or imbrication in redbeds, which are the most studied sedimentary formations in Asia (e.g., Dupont-Nivet et al., 2002; Gilder et al., 2003; Tan et al., 2003, 2010); (2) a large geomagnetic field anomaly during the Cenozoic of whether regional (e.g. Chauvin et al., 1996) or global origin, with significant amount of non-dipolar components in the Cenozoic magnetic field (e.g. Si and Van der Voo, 2001); (3) an ill-understood and nearly unknown deformation of the Eurasia plate allowing eastern Asian regions to be located some ~10° farther south than expected during the Cenozoic (e.g. Cogné et al., 1999; Hankard et al., 2007a).

Although each of these mechanisms has been widely debated, no general and detailed

analysis of the whole Meso-Cenozoic paleomagnetic database has yet been proposed, although it could help deciphering main trends of this anomaly over Asia. We thus propose such an analysis of the Meso-Cenozoic paleomagnetic database, from which we discuss consequences on several key-points such as the locus and age of India collision with Eurasia, the intracontinental deformation due to India indentation, the amounts of convergence/divergence between continental blocks, the hypothesis of a postulated single, large rigid Eurasia Plate since the Cretaceous and the appropriateness of the Europe APWP to analyze Asian data, and the dipolar magnetic field geometry hypothesis.

2. Compilation of Meso-Cenozoic paleomagnetic data.

In order to unravel the inclination anomaly in Asia, we present a new compilation of previously published Meso-Cenozoic paleomagnetic data based on the following : (1) a selection of results from the Global Paleomagnetic Database of McElhinny and Lock (1996), update 2004 (GPMDB-04) using keywords "continent"=Asia, "low age" = 0 and "high age" = 175; this selection resulted in a list of 829 paleopoles; (2) a publication search using *ISI Web of Sciences* for 2004-2008 with keywords "Asia" and "paleomagnet*" which resulted in a list of 113 paleopoles amongst which 80 are younger than 175 Ma. At this first stage, we thus obtained a total of 913 poles, 620 derived from sedimentary rocks (mainly red sandstones), while the remaining 293 are from igneous rocks (mainly effusive rock formations).

Although we aim at using a maximum number of data in order to highlight the overall trend of the inclination anomaly, we made further selections on this database (Fig. 1a): (1) we excluded 136 data coming from remote localities which we considered as being situated too far away from our area of analysis; these extend from India in the south to Siberia in the north, and western Central Asia in the west to eastern Siberia in the east. (2) In GPMDB-04, there are a number of combined results which average similar results from a given region; these combined results, considered as redundant with respect to originally published data, have been excluded from our compilation. (3) Finally, poor quality data, characterized by confidence angles *A95* or *dp* larger than 15° have also been discarded. Sorting criteria (2) and (3) led us to reject 244 lines in our database.

These various selections finally end up with 533 independent paleopoles (Fig. 1a), 374 obtained from sedimentary rocks, 159 from igneous rocks (Table A1 in *online supplementary material*), extracted from 278 references published prior to date (Table A1 and A2 in *online supplementary material*; all 278 references are provided in *online supplementary material*). We finally sorted these data into 2 groups, depending on the sedimentary or igneous nature of

the sampled rock formations, and distributed them over 18 blocks or terranes as usually defined in the Asian mosaic (e.g. Enkin et al., 1992; Chen et al., 1993b; Halim et al., 1998a etc.. Table A1; Fig.1a): Siberia (SIB), Amuria (AMU), North China Block (NCB), South China Block (SCB), Korea peninsula (KOR) and Japan (JAP) for northeastern regions, Indochina (INC) defined in 3 areas: Malaysia-Burma (MB), Simao Terranes (ST) and Khorat Plateau (KH) in southeast Asia, Lhasa (LH), Qiangtang (QI) Kunlun (KUN) and Qaidam (QA) blocks in Tibet, Jungar (JUN), Tarim (TAR) and Kazakhstan (KAZ) blocks in Central Asia, and finally India (IND) in the south, and Middle East Asia (MEA) terranes (from Tadjikistan, Turkmenistan, Turan etc..) in the west.

The spatial and temporal distributions of data are illustrated in Fig. 1. They deserve several remarks: (1) data are not evenly distributed either in space (Fig. 1a), or time, nor even in rock type (Fig. 1b and c). (2) In effect, we first notice that the number of results obtained from sedimentary rocks is more than twice as large as that deduced from igneous rocks (Table A2). This point must be kept in mind, since sedimentary processes such as compaction are often advocated as a major cause for inclination flattening, hence anomaly, in the region. (3) Apart from India data, there is a clear tendency in the distribution of igneous rock localities (Fig. 1a) over northeastern stable (?) regions SIB, AMU, NCB, SCB, KOR and JAP. In contrast, Central Asia and Southeast Asia data were obtained predominantly from sedimentary rock localities, because of effusive rocks outcrops scarcity. This point is also important, because these regions are suspected to be mobile one to each other and with respect to Siberia. Therefore, the inclination variations due to N-S relative movements linked to the Asia deformation are superimposed on a possible inclination shallowing due to sedimentary flattening effects. (3) Finally we note that a large part of the Tertiary era (e.g. ~60-20 Ma; Fig. 1b and c) is particularly poor regarding the number of results, which may somewhat render uneasy the characterization of this anomaly during this critical period.

3. Description of the paleolatitude anomaly

3.1. Definition of the paleolatitude anomaly

We now turn to a description of the inclination anomaly, in terms of paleolatitude anomaly. In effect, there are 2 ways to describe the anomaly: either (i) by comparing experimentally defined paleomagnetic inclination at a given site location with the inclination one should obtain at this locality from the position of a reference pole from a reference APWP, or (ii) by comparing the angular distance between observed and expected paleopoles after correction for possible local rotation of the site around a vertical axis. The latter is

simply the angle between the 2 paleo-equators (observed vs. expected), or, equivalently, the difference between the observed paleolatitude for a given age at a given place and the paleolatitude which can be computed at that locality from the relevant reference APWP paleopole (Fig. 2). We therefore define the paleolatitude difference as $\{\Delta\lambda = p\lambda_{obs} - p\lambda_{exp}\}$. where $p\lambda_{obs}$ is the actual paleolatitude from our selected database (Table A1), and $p\lambda_{exp}$ the expected paleolatitude at each locality as computed from the relevant reference poles of the Europe APWP. For every paleopole, this difference was computed at its age, rounded to the 5 Ma closest reference pole, notwithstanding its age uncertainty. The uncertainties around $\Delta\lambda$ have been computed from 95% confidence intervals of both reference and observed paleopoles, following the procedure of Coe et al. (1985). A negative $\Delta\lambda$ indicates shallow inclinations, or anomalously south paleopositions of the locality with respect to the reference APWP, whereas a positive $\Delta\lambda$ implies steep inclinations, or anomalously north paleopositions with respect to the reference.

We have computed $p\lambda_{exp}$, the expected paleolatitude at each point, using reference poles of Europe APWP of Besse and Courtillot (2002, hereafter referred as BC02; Fig. 3, Table A1). We did not use the more recent APWP of Torsvik et al. (2008; hereafter referred as T08) because comparison of Europe BC02 and T08 APWPs reveals minor differences, since they are based on quite similar databases. As a matter of fact, the angles between pairs of reference poles of a given age from both curves are always statistically insignificant, lower than a maximum value of 5.3° ± 5.8°, with an average of 2.7° ± 1.3°.

3.2. Maps of paleolatitude anomaly - reference: Europe APWP.

As a first step of analysis, we constructed a map of the paleolatitude differences computed as $\Delta\lambda = p\lambda_{obs} - p\lambda_{exp}$, as defined above. Data older than 50 Ma from India were discarded since this continent was probably not yet amalgamated to Eurasia prior to this age. Similarly, all the data older than 140 Ma have not been included in the computation of these anomaly maps, because of the ~130 Ma age closure of the Mongol-Okhotsk ocean, before which all eastern Asian blocks have not yet amalgamated with the Eurasia continent (Kravchinsky et al., 2002; Cogné et al., 2005; Hankard et al., 2007b; van Hinsbergen et al., 2008; Metelkin et al. 2007, 2010; Kovalenko, 2010). The 422 remaining data collection (Table A3 in *online supplementary material*) have been splitted into 2 groups: a roughly Cretaceous-Eocene 140-50 Ma-old collection (Fig. 3a; n=240) and a Cenozoic group, 50-0 Ma-old collection (Fig. 3b; n=182). We then applied a smoothing technique by computing

average $\Delta\lambda$ at each discrete point of a grid defined by nodes every 5° in latitude and longitude (crosses in Fig. 3) on which are centered circular windows of 5° 1/2 aperture angles. Finally note that these maps have been constructed by mixing all the rock types, sedimentary and igneous (Table A4 in *online supplementary material*). This will be discussed in section §4.2.

In the anomaly maps shown in Fig. 3, cold colors (green to blue) indicate positive paleolatitude differences $\Delta\lambda$, hot colors (yellow to red) point out negative $\Delta\lambda$. The 140-50 Ma map (Fig. 3a) displays large amplitudes of $\Delta\lambda$ variations, ranging from -22° to +20°. We first note an area of positive $\Delta\lambda$, up to 13°, in NW Siberia, around {60°N, 85°E}. However, this positive anomaly is defined by only 4 data, coming from quite old paleomagnetic studies (poles Id# 1112 to 1115 in Table A1). Therefore, we will not further discuss this positive anomaly, because of the suspected poor quality of data (demagcode=2). Turning to remaining anomalies, their distribution over Asia well reflects the generally admitted interpretations of paleomagnetic data from these regions. We underline 3 contrasted areas (Fig. 3a): (1) yellow-orange to light green areas covering the KAZ region and a large part of east Asia, from SIB to SCB, point to a near-zero paleolatitude difference between observed and predicted paleolatitudes. This supports the idea that the BC02 Europe APWP can be used as a reference for the paleoposition of Siberia, at least during the Cretaceous, and that there has been no significant N-S relative movements between KAZ, SCB, NCB, AMU and SIB since that time. (2) An orange-red anomaly is located on Tibet and Central Asia, indicating largely distributed negative paleolatitude differences. This has long been interpreted (generally based on shallow inclination observations) as resulting from northward motion of these areas with respect to Siberia under the effect of ongoing penetration of the Indian plate into Asia since its post-Cretaceous collision (e.g. Achache et al., 1984; Besse et al., 1984; Chen et al, 1992, 1993a, 1993b; Halim et al., 1998a; Cogné et al., 1995). (3) The Southeast Asia peninsula is characterized by green to blue colors corresponding to a positive paleolatitude anomaly (or steep inclinations), up to 16°-18°. Classically interpreted in terms of tectonic movements, this reveals a large post-Cretaceous southward movement of these blocks or terranes with respect to Siberia, due to lateral extrusion of SE blocks under the effects of the India collision and penetration into Eurasia (e.g. Yang and Besse, 1993).

Contrasting with this simple figure, the 50-0 Ma map (Fig. 3b) exhibits a completely different distribution of anomalies. In effect, almost all the map is covered with orange-red colors, indicative of an overall negative paleolatitude anomaly over Asia. This anomaly can be quite high, up to more than -15° to -20° in several places such as eastern (Qaidam area)

central (Lhasa) and western (Pamir) Tibet. Moreover, a significantly negative $\Delta\lambda$ is also observed in the eastern blocks such as NCB, KOR, SCB and AMU. In a simple tectonic interpretation, this would suggest not only that Tibet and Central Asia would have largely converged with Siberia (more than 15°) during the Cenozoic, but also that eastern blocks would have significantly converged with Siberia. Because Cretaceous paleolatitudes of the eastern blocks are consistent with the Europe APWP, this convergence should have been preceded by a N-S episode of rifting. This, indeed, is completely inconsistent with our understanding of Asian tectonics, and this map provides a further illustration of what is known as the Tertiary inclination anomaly in Asia.

3.3. Anomaly of northeastern stable blocks/terranes.

After this first overview, we now discuss paleolatitude anomalies in a more detailed way. In Figures 4 and 5 we provide illustrations of $\Delta\lambda$ as a function of age for 5 different blocks: AMU and SIB (Fig.4), NCB+KOR and SCB (Fig.5).

First examining data from the Amuria block (Fig. 4a), it is important to note that (1) 27 out of the 29 data from this block are from igneous rocks (solid dots), and (2) most of these data result from quite recent and high quality studies (Table A1). In this plot, we may distinguish 3 time periods, separated by large grey hatched lines in Fig. 4a: (1) a large discrepancy of 20°-40° between expected and measured paleolatitudes in the late Jurassic. This indeed indicates that the Mongol-Okhotsk Ocean is still widely opened, as described by Kravchinsky et al. (2002) and Cogné et al. (2005). (2) Between ~130 Ma and ~70-60 Ma, $\Delta\lambda$ data are distributed around the zero line, which reinforces the idea that the Amuria, hence Siberia, Cretaceous paleolatitude is well predicted by the BC02 Europe APWP. This is, on another respect, well demonstrated by all recent paleomagnetic results from these northern areas (Kravchinsky et al., 2002; Cogné et al., 2005; Hankard et al., 2007b; van Hinsbergen et al., 2008; Metelkin et al., 2007, 2010; Kovalenko, 2010). (3) Finally, since at least 60 Ma and up to 15-20 Ma, $\Delta\lambda$ are systematically negative, although they are derived from igneous rocks. This describes the "Tertiary inclination shallowing anomaly", and therefore confidently suggests that this anomaly is not primarily due to sedimentary processes-induced flattening mechanisms in sediments, as pointed out by Cogné et al. (1999) or Hankard et al. (2007a). The grey strip drawn over points in Fig. 4a qualitatively underlines this 3 stages evolution.

Turning to Siberia data (Fig. 4b), we first note that data are dominantly obtained from sedimentary rocks (18 out of 27), and studies are in general older than for other regions of

Asia (Table A1). This might be partly responsible for the large scatter of data with, in particular, the 4 anomalous points at 123 Ma resulting in the positive anomaly of NW Siberia described in Fig. 3a (section §3.2). Moreover, there is a large gap in the database between 70 Ma and 20 Ma. However, main observations made on the Amuria block still hold: the observed Cretaceous paleolatitudes are roughly consistent with the expected ones, and the 4 late Cretaceous/Eocene data display paleolatitudes which are significantly lower than expected. Indeed, there is also a difference between Siberia and Amuria in the late Jurassic data, since Siberia is the northern edge of the Mongol-Okhotsk Ocean, and Amuria its southern edge at that time.

NCB, KOR and SCB (Fig. 5a and b) provide a much larger number of data, with a larger amount of data from sediments: 60% in NCB, 90% in SCB. At first sight, however, there is no clear trend revealing that the anomalies in sedimentary rocks are systematically larger than those from igneous ones. As underlined by the (qualitative) grey strips drawn in the plots of Fig. 5a and b, the point distributions appear very similar to that of Amuria (Fig.4a): an overall consistency of the expected vs. measured paleolatitudes in the Cretaceous, and a systematic negative $\Delta\lambda$ anomaly during the Cenozoic, with respect to the Europe APWP.

At this stage, we conclude that if the BC02 Europe reference APWP properly describes paleopositions of Siberia, Amuria, the North and South China blocks and the Korea peninsula during the Cretaceous, there is a systematic bias of about 10-15° between the expected and observed paleolatitudes in these blocks in the Tertiary. In other words, the reference Europe APWP does not predict the paleopositions of this stable part of Eurasia in the Cenozoic. Thus, in the following, we attempt to define a new Meso-Cenozoic reference APWP for East Asia, based on the actual paleomagnetic results from this region.

4. A new Meso-Cenozoic reference APWP for East Asia.

4.1. computations and results.

Before going further into details about the cause of this discrepancy between the observed and expected paleolatitudes of northeastern asian regions in the Cenozoic, we first propose to compute a 0 Ma to 130 Ma APWP solely based on data from Siberia, Amuria, the North and South China blocks and the Korea peninsula (Fig. 6a), as listed in Table A1, and importantly, under the basic hypothesis of a dipolar magnetic field. Concerning the geological ages, we have used ages as given in the GPMDB04 database for most of the paleopoles. When a pole is referred to a stratigraphic age (e.g. "lower Cretaceous", "Paleogene", etc…)

we have used the Gradstein et al. (2004) timetable in order to assign a central window age, with its lower and upper limits. When published articles provide radiometric ages, we have used these ages with their experimental uncertainties.

Because of similarities in the anomaly between these blocks (Fig. 4 and 5) we consider this group of blocks as forming a single entity in the Meso-Cenozoic, which we will use as a reference to analyse the relative movements of other blocks constituting the Asian mosaic. Indeed we limited this curve to 130 Ma, because of the Late Jurassic/Early Cretaceous closure of the Mongol-Okhotsk Ocean separating Siberia from all other blocks. Thus, the APWP we propose, the so-called East Asia APWP, is based on a total of 146 paleopoles listed in Table A1, 66 (45%) from igneous rocks, and 80 (55%) from sediments distributed over the cited blocks (Table A5 in *online supplementary material*, Fig. 6a). We constructed this APWP by averaging paleopoles every 10 Myr, with variable sliding window widths of 20 and 40 Myr. A window width of 20 Myr was used for the 0 to 20, and 100 to 130 Ma mean poles. Because of the need to compensate for the small number of data in the Tertiary (e.g. Fig. 1b and c) and to smooth large dispersions of data, mainly due to local tectonic rotations, a 40 Myr window width has been used for the 30 to 90 Ma poles.

In effect, although we consider the assemblage of these blocks and terranes as stable since the Late Jurassic/Early Cretaceous closure of the Mongol-Okhotsk Ocean, on the basis of paleolatitudes analysis (section §3, above), the Tertiary tectonics due to the India collision with Eurasia is active allover Asia, and may produce local rotations along faults which deviate the paleopoles from their initial location along small-circles. Such rotations have been reported at several localities from all blocks or terranes from these eastern regions: Siberia and Mongolia (e.g. Halim et al., 1998b; Cogné et al., 2005; Otofuji, 1995, 2006), NCB and SCB (e.g. Funahara et al., 1992; Gilder et al., 1993b; Huang et al., 2007), Korea peninsula (e.g. Lee et al., 1999; Park et al., 2005), amongst others. These rotations result in a small-circle distribution of paleopoles as illustrated for the 20, 50 and 100 Ma paleopoles in Fig. 6 (b, c and d, respectively), where best-fit small-circles (Mardia and Gadsden, 1977), centered on the average site locations, are drawn over the point populations. Thus, these small-circles represent the average distance of the sites from the north pole, their mean paleocolatitude. However, for the sake of constructing an APWP, we need to calculate mean paleopoles. We have computed them as the mixed averages between fixed paleopoles and small-circle passing through paleopoles which are suspected to be rotated (so-called "free to rotate" poles by Besse and Courtillot, 2002) and centered on the site location (square symbols in Fig. 6b to d). These mixed averages, routinely implemented in *PaleoMac* (Cogné, 2003), were computed using an

algorithm similar to McFadden and McElhinny (1988) in the case of mixed averages between data points and great-circles, where rotated poles are given a 0.5 weight, as compared to the 1.0 weight of fixed poles, for computing the α_{95} confidence areas around the means.

We underline that if some paleopoles can be unequivocally considered as rotated due to local tectonics (e.g. Fig. 6c) or confidently interpreted as rotated (Fig. 6b), some situations appear more ambiguous (Fig. 6d), where the whole population appears elongated, without a clear cluster of unrotated paleopoles which could serve as a reference. In such case, we relied on the vicinity of active faults as described in the original publications, to hypothesize suspected rotations. For example all the free-to-rotate paleopoles at 100 Ma (Fig. 6d), except from the largely counterclockwisely rotated one from Amuria (Otofuji et al., 2006), come from Korea Peninsula, where active Cenozoic faulting is described (e.g. Park et al., 2005). Altogether, however, we conclude that these possible uncertainties may affect the azimuth of mean paleopoles as viewed from site locations, but not the north pole distance from (or paleocolatitudes of) sites, as obvious from the good consistency between these mean paleopoles and the small-circle path over point populations (grey strips in Figs. 6b to d).

This new East Asia APWP (Table 1) is compared to the BC02 Europe APWP (open dots), and displayed with (Fig. 6e) and without (Fig. 6f) A_{95} circles of confidence for the sake of clarity. As analyzed above, there is a clear discrepancy between the 2 curves in the Cenozoic. This difference is statistically significant up to 60 Ma. From 70 to 130 Ma, although there are some angular differences between poles from the 2 curves, they are not statistically different, except for the pole at 130 Ma, but this difference could arise from the uncertainty induced by the mixed average we used, due to possible local rotations as discussed above. This kind of uncertainty may also affect the Tertiary poles of our curve. However, these possible rotations do not affect the significant difference in the Cenozoic parts of the 2 APWP. In effect, computation of small-circles passing through the 10-60 Ma poles of both Europe (Besse and Courtillot, 2012) and East Asia (present study) APWP's reveals an average paleolatitude difference of 9.4° ± 1.9° for an arbitrary reference point located in East Asia at {45°N, 120°E} (Fig. 4f). This difference is in full agreement with our analysis of section §3.3 above, where the East Asia stable blocks appear to have a lower paleolatitude than expected from the Europe APWP.

4.2. East Asia APWP and checking for flattening in sediments.

In order to evaluate the validity of this new East Asia reference APWP, we propose 2 tests. The first one consists in re-computing the $\Delta\lambda$ differences of the 146 data used to

construct the APWP, using this new APWP as a reference (Table A1) and sorting data into 2 sub-sets: sedimentary rocks (n=80, Fig. 7a) and igneous rocks (n=66, Fig. 7b). We computed the mean deviations of $\Delta\lambda$ from 0 to 150 Ma, by three 50 Myrs time periods (Fig. 7). As expected, both populations of sedimentary and igneous rocks show insignificant deviations which average around $\Delta\lambda = 0°$, with $\Delta\lambda < \pm 1°$ and uncertainties of the order of ~6°-7° in both populations, with a possible, larger mean $\Delta\lambda = -3.2° \pm 7.3°$ for 0-50 Ma sediments. This negative difference is what one would have expected from sedimentary inclination flattening processes, but accounting for the large natural scatter of data, as underlined by the large confidence area, this result does not appear as significantly different from zero. Thus, an overall systematic bias of the sedimentary data towards negative $\Delta\lambda$ values resulting from inclination flattening, cannot be demonstrated.

The same conclusion holds for a second test held on data from Japan (Fig. 8), which we did not include in East Asia APWP computations, and thus are totally independent from this new APWP. Computation of $\Delta\lambda$ using the Europe APWP as a reference (Fig. 8a) clearly leads to negative $\Delta\lambda$ which tend to increase with age up to 20 Ma, following the trend described for the other East Asia blocks. This should erroneously lead to the conclusion that Japan islands have suffered from a northward movement, as large as ~10° since 20 Ma (Fig. 8a), relative to Siberia, in total contradiction with the north-south opening of the Japan Sea, as proposed by Jolivet et al. (1994). In effect, this would have resulted in a southward motion of Japan of few hundreds of kilometers (~<500 km). As mentioned previously, this negative $\Delta\lambda$ affects igneous rocks as well as sediments. In contrast, when using the new East Asia APWP as a reference (Fig. 8b), this discrepancy vanishes, and $\Delta\lambda$ averages at $-0.9° \pm 4.7°$ for the whole population (n=40) with, here again, an insignificant difference between sediments (mean: $\Delta\lambda = -2.0° \pm 5.2°$, n=15) and igneous rocks (mean: $\Delta\lambda = -0.2° \pm 4.3°$, n=25). This demonstrates (i) the lack of any significant ~~N–S~~ southward movement of Japan relative to Siberia, that could have been suggested when using Europe APWP as a reference and (ii) concerning magnetization acquisition in sediments, we reach the same conclusions as above: no systematic significant bias of sedimentary rocks data can be put forward on Japan dataset, in terms of a flattening of paleomagnetic inclination due to sedimentary processes such as compaction.

Here, we therefore reach an important conclusion: although it can be advocated in some particular studies (e.g. Bazhenov and Mikolaichuk, 2002; Dupont-Nivet et al., 2002; Tan et al., 2003, 2010; Gilder et al., 1996, 2001, 2003, 2006; Tauxe and Kent, 2004; Yan et

al., 2006, amongst others), and what could be the dominant cause(s) for "Cenozoic Inclination Anomaly" in Asia, a paleomagnetic inclination shallowing due to diagenetic and compaction processes in the sediments deposition and lithification is probably not a major cause of the observed large scale inclination anomaly problem in Asia.

5. Implications on the Cenozoic tectonics of Asia.

5.1 Maps of paleolatitude anomaly - reference: East Asia APWP.

Still before deciphering main causes of discrepancies between the Europe APWP and our new East Asia APWP, we now briefly examine the implications of this new East Asia reference in terms of evaluation of intracontinental shortening and lateral extrusion of the Asian blocks due to the India plate collision.

We computed new maps of $\Delta\lambda$ anomalies, calculated as $\{\Delta\lambda = p\lambda_{obs} - p\lambda_{exp}\}$, where $p\lambda_{obs}$ and $p\lambda_{exp}$ are the observed and expected paleolatitudes respectively, as described in section §3.2, but using our new APWP for East Asia as a reference (Fig. 9). As one would expect, the 140-50Ma map of $\Delta\lambda$ (Fig. 9a) based on our new reference APWP does not differ significantly from the map we obtained using the BC02 Europe APWP (Fig. 3a). This, indeed, is due to the fact that the APWP poles from Europe on the one hand, and East Asia on the other hand, are indistinguishable at a statistical level for ages older than ~60-70Ma (Fig. 6). Thus, the expected paleolatitudes ($p\lambda_{exp}$) computed using either of these reference paths are quite similar (Table A1), and consequently, the $\Delta\lambda$ anomalies show very similar patterns (Fig. 3a and 9a).

In strong contrast, the 50-0 Ma $\Delta\lambda$ anomalies map computed with the East Asia APWP (Fig. 9b) shows a significantly different result than the one we obtained using the BC02 Europe APWP (Fig. 3b). Three areas can be clearly distinguished: (1) a north-eastern area, dominated by yellow to light green colors, where, logically, paleolatitude anomalies are confined around zero (±5°, typically) demonstrating the lack of relative paleolatitudinal movements between these blocks and terranes (SIB, AMU, NCB, KOR and SCB), as generally recognized from tectonic studies. (2) A southeastern area, dominated by deep-blue colors, which denote a southward movement of these terranes, up to ~12.5° to 15°, with respect to stable eastern blocks since, at most, 50 Myr. This, indeed, is in very good agreement with the southeastward Asia extrusion model of Molnar and Tapponnier (1975), Tapponnier and Molnar (1979), Tapponnier et al. (1986), for example. The quantitative amount of extrusion, which can be derived from paleomagnetic data, is further discussed

below. (3) Finally, a large central/western area, including all the Tibet and Central Asia blocks still exhibits warm orange-red colors, which may be tectonically interpreted as resulting from a significant northward motion of these blocks with respect to Siberia, thus reflecting the intracontinental shortening between India and Siberia since the time of collision. It should be noticed that this map (Fig. 9b) demonstrates at most ~10°-15° of continental shortening (from western India to north-eastern Tibet, i.e. the Qaidam block), a more reasonable value than the ~15°-25° shortening implied by the $\Delta\lambda$ anomaly map obtained when using the BC02 reference Europe APWP (Fig. 3b). Overall, this observation is also in good agreement with the suspected post-Cretaceous continental shortening amounts as published in the last two decades (e.g. Enkin et al., 1992; Chen et al., 1993a, 1993b; Halim et al., 1998a, amongst other).

This analysis clearly reveals that the Cenozoic "Inclination Anomaly" is actually twofold: (1) on the one hand, a part of the anomaly in Asia is likely due to the post-India collision tectonics resulting in relative latitudinal movements between Siberia, Tibet, Central and Southeast Asia blocks, which appears as a 2nd-order anomaly; (2) on the other hand, a general "regional" trend of shallow Cenozoic magnetizations, or shallow paleolatitudes, over all Asia is superimposed on these "local" anomalies, which we propose to name the 1st-order anomaly. Before trying to decipher the causes for the latter overall trend, discussed hereafter in section §6, we now turn to a reappraisal of intracontinental tectonics, comprising shortening in Central Asia, and lateral extrusion of continental segments, as deduced from the so-called 2nd-order anomaly.

5.2. Reappraisal of Tibet and Indochina vs. Siberia post-Cretaceous relative movements.

We have thus re-computed (Table A1) $\Delta\lambda$ paleolatitude anomaly, using East Asia APWP (present study; Table 1; Fig. 6) as a reference for all mobile blocks from Tibet, Central Asia, and southeast Asia, situated north and east of the India indentor into Asia. Beginning with all Tibetan blocks, Lhasa, Qiangtang and Kunlun (Fig. 10a), and not surprisingly, our computations lead to a post-Cretaceous convergence with Siberia which amounts to 11.3° ± 9.2° (1250 ± 1020 km; solid black line with grey uncertainty in Fig. 10a), or solely when based on the Lhasa block data, to 13.2° ± 8.5° (1450 ± 940 km; hatched bold line in Fig. 10a) of post-Cretaceous intracontinental shortening between the southernmost parts of Tibet and the northernmost parts in Amuria/Siberia. These values appears to be slightly lower than the previously published estimates of ~1700 to 2000 km of post-Cretaceous intracontinental

shortening (e.g., Achache et al., 1984; Lin and Watts, 1988; Chen et al., 1993b; Patzelt et al., 1996; Liebke et al., 2010; Sun et al., 2010, 2012; Table 2) between south Tibet and Siberia.

After correction from the 1st-order anomaly, Tibet convergence with Siberia during the Cenozoic may be evaluated, using the East Asia APWP as a reference for Siberia, at 6.0° ± 3.6° (670 ± 400 km; Fig. 10a). This value is, indeed, more conceivable than the one deduced from a comparison of actual paleomagnetic results with those expected from the BC02 reference curve. Moreover, it is corroborated by the recent results of Lippert et al. (2011) from Qaidam Paleogene effusive rocks (note that this recent result is shown in Fig. 10a, but not included in computations). Importantly, we finally stress that no particular bias between sedimentary (open symbols) and effusive (closed symbols) rocks data prior to 50 Ma is obvious from these results from the Tibet blocks (Fig. 10a). A large scatter of data is obvious, but it does not clearly appear to pertain to the magnetization acquisition mechanisms, even though some particular sedimentary results could have been affected by inclination shallowing mechanisms, as debated by Tan et al. (2010).

Turning now to the southeast, the other extreme end of this N-S relative movements system, results from the Indochina peninsula (Fig. 10b) appear in cold green to blue colors in anomaly maps of Fig. 3a, 9a and 9b, exhibiting systematic positive $\Delta\lambda$ or inclination anomalies. This positive anomaly is the evidence that in these regions, the Cretaceous, as well as the Cenozoic inclinations are steeper than the ones expected and deduced from the BC02 Europe, or the present East Asia APWPs. Thus, in terms of paleolatitudes, these results point to a Cenozoic southward motion of this area with respect to the Siberia craton. Our compilation results in a southward post-Cretaceous motion of Indochina with respect to Siberia, using our reference East Asia APWP, of 4.3° ± 6.6° (480 ± 730 km), and a Cenozoic value of 2.4° ± 5.0° (270 ± 550 km). These weak values are statistically insignificant. However, they do not contradict tectonic models of southeastward extrusion of Indochina along major shear-zones such as the left-lateral Red River fault zone (e.g. Leloup et al., 1995), which has been estimated to be as large as 1200 ± 500 km (Yang et al., 1995) to 1500 ± 800 km (Yang and Besse, 1993) of motion along the fault, from a comparison of Mesozoic paleomagnetic results from Indochina and South China blocks.

Nevertheless, the comparison of datasets from the Lhasa block and Indochina (Fig. 10a and b), using the East Asia APWP, clearly reveals significant relative N-S (Lhasa towards the north, Indochina towards the south) amounts of post-Cretaceous 17.5° ± 8.6° (1950 ± 950 km) to Cenozoic-Present 8.4° ± 4.9° (930 ± 540 km) relative paleolatitudinal movements. Although our analysis cannot provide exact amount of Indochina extrusion, comparison of

paleomagnetic data from the Lhasa block and Indochina unequivocally suggests a southward out-of-Cretaceous-Asia extrusion of Indochina peninsula in the Cenozoic. Finally, it should be noticed that although it is consistent with the extrusion models, our analysis does not allow to provide conclusive support to the controversy about large (e.g. Molnar and Tapponnier, 1975; Tapponnier and Molnar, 1979, Tapponnier et al., 1982, Replumaz and Tapponnier, 2003; Yang and Besse, 1993) vs. small, or unnecessary (e.g. Dewey et al., 1988; Hall et al., 2008), amounts of extrusion.

5.3. Central Asia blocks vs. Siberia relative movements.

The situation here is less easy to describe (Fig. 11), mainly because the data collections are dominated by a large number of results obtained from sedimentary rocks, 28 out of 29 total data from Qaidam (Fig. 11a), and 27 out of a total dataset of 30 results from the Tarim and Jungar blocks (Fig. 11b). Sedimentary results are subject to 2 types of suspicion: (1) sedimentary processes-induced inclination shallowing, and (2) possible age determination errors in these (dominantly) red formations. We further underline that the idea of inclination shallowing in sediments is reinforced by a systematic weak $\Delta\lambda$ discrepancy with reference APWP of very sparse (4 out of 59 data points) effusive rocks data from Qaidam (Sun et al., 2006; Fig. 11a), Tarim (Gilder et al., 2003; Huang et al., 2005; Fig 11b) and Jungar (Huang et al., 2006; Fig. 11b). Acknowledging a purely sedimentary processes origin of inclination shallowing in these regions would, however, imply a near-zero convergence of these areas with Siberia since the Cretaceous, which contradicts the Cenozoic intracontinental shortening demonstrated by structural geologists and tectonophysicists (e.g. Meyer et al., 1996, 1998; Métivier et al., 1998; Pei et al., 2009), based on analysis of the Cenozoic mountain chains building between various blocks (e.g. Tien Shan, Altay and Qilian Shan ranges).

The Pre-Cenozoic $\Delta\lambda$ paleolatitude anomaly of Central Asia is systematically negative, averaging -11.9° ± 8.0° in the Qaidam block (Fig. 11a) and -9.7° ± 5.5° in Tarim + Jungar (Fig. 11b). Taken at face values in the hypothesis of a purely tectonic cause, these would be interpreted as a post-Cretaceous 1320 ± 890 km convergence of Qaidam with Siberia, and a 1080 ± 610 km Tarim+Jungar convergence. These values appear somewhat too large with respect to intracontinental shortening estimates (e.g. less than 200 km in Tien Shan range proposed by Avouac et al., 1993). We thus stress that these values are only indicative, but accounting for their large error bars, they appear to be still quite consistent with reconstructions we propose in the next section (§6, Fig. 14).

Analysis of Cenozoic data is even less straightforward. An attempt of estimating the convergence of Qaidam with Siberia during Cenozoic times faces two problems: (i) inclination shallowing in sediments (no effusive rocks data) together with (ii) possible age errors. In effect, the 0-10 Ma data (marked *(e)* in Fig. 11a) are excluded from the average estimates, because of a suspected 10 Myrs age error. Consequently, only results from the 50-10 Ma window are included in the average $\Delta\lambda$ computation displayed in Fig. 11b. This average $\Delta\lambda$ provides a discrepancy of -10.3° ± 4.5°, implying a 1150 ± 500 km convergence of Qaidam and Siberia (Fig.11a). Here again, these values appear as overestimated, albeit in the right sense, with respect to the reasonably well understood amounts of intracontinental shortening north of Tibet, and might result from significant inclination shallowing effect of sedimentary processes. Finally, the paleomagnetically-based convergence of Tarim and Jungar blocks toward Siberia (Fig. 11b) cannot be demonstrated, due to the large scatter of data.

We thus conclude here that the $\Delta\lambda$ paleolatitude anomaly observed in Central Asia (Tarim, Qaidam, and Jungar) remains rather inaccurate in providing estimates of the intracontinental shortening between India and Siberia, within Central Asia, because of the scarcity of effusive data and the suspicion of inclination shallowing in sediments. However, we underline that using the East Asia APWP reduces the Cenozoic inclination anomaly by more than a factor 2 in these regions, with respect to previously proposed values as based on the BC02 reference APWP for Europe.

5.4. Insights on India collision with Asia and Asia intracontinental shortening.

Our new East Asia APWP has finally strong consequences on the age and place of the India collision with Asia. The locus and time of collision of India with Asia are still currently objects of hot debates. Based on paleontological arguments, Jaeger et al. (1989) proposed a contact age close to the Cretaceous/Tertiary boundary at ~65 Ma, from similarities between Eurasia and India terrestrial faunas at that time. However, this solution would imply an intracontinental convergence of India with Siberia larger than ~4000 km. More weight is given to the approach of Patriat and Achache (1984), based on the analysis of magnetic isochrons of Indian Ocean, which point to a drastic slowdown of India plate velocity at ~55 Ma, supposed to occur as an aftermath of the Tethys ocean closure and India collision. This was later confirmed by a reappraisal of these anomalies and kinematic parameters by Royer and Patriat (2002) and Copley et al. (2010). This idea was then confirmed by numerous

paleomagnetic studies and syntheses (e.g. Besse et al., 1984; Enkin et al., 1992; Chen et al., 1993b; Patzelt et al., 1996; Halim et al., 1998a), which suggested a collision latitude of 10-15°N, followed by a total convergence of India and Siberia on the order of ~2700-3000 km, up to ~3500 km.

Owing to a collision age at ~50-60 Ma at low latitudes (e.g. ~10-15°N), the synthetic reference APWP curves of India and Eurasia (e.g. Besse & Courtillot, 2002) predict a post-collisional convergence of 2700 to 3500 km between the present-day northern edge of India plate, and Siberia. This large paleolatitude difference would have been subsequently absorbed into an intracontinental shortening within two major zones: (i) a northern continental extension of India called "Greater India" (e.g. see a review in Ali and Aitchison, 2005 and van Hinsbergen et al., 2012), and (ii) throughout Central Asia terranes, from Lhasa, Qiangtang and Kunlun blocks from Tibet to Siberia. Numerous paleomagnetic studies and syntheses have proposed various estimates of both the pre-collisional Greater India northern extent, and the total Lhasa/Siberia shortening amounts, and their distribution throughout Tibet, in Lhasa, Qiangtang and Qaidam blocks, and the reactivated mountain chains such as Kunlun, Tien Shan and Altay ranges.

We propose a synthesis of main published estimates of the total India/Siberia and Lhasa/Siberia convergences, and of the Greater India extent in Table 2. There are two tendencies: (1) On the one hand, some authors assume a more recent collision age, lower than ~45 Ma, and as young as 34 Ma, at higher paleolatitudes, greater than ~22°N (e.g. Aitchison et al., 2007; Tan et al., 2010; Dupont-Nivet al., 2010a). The solution of Aitchison et al. (2007), however, has been disputed on geological and paleomagnetic grounds by Garzanti (2008) and Najman et al. (2010). (2) On the other hand, recent paleomagnetic studies held on either igneous (Liebke et al., 2010; Sun et al., 2010) or sedimentary (Yi et al., 2011; Sun et al., 2012) rock formations from the Lhasa terrane, confirm low paleolatitudes (~10-15°N) and older ages (49-55, up to 65 Ma, Table 2) for the collision, as earlier proposed by Besse et al. (1984) and Patzelt et al. (1996). However, these studies still face the necessity of a 1400-1900 wide Greater India and a ~1500-2000 km intracontinental shortening in Central Asia to account for a post-collisional India/Siberia convergence in excess of ~3000 km.

In order to point out our contribution to this problem, we have computed paleolatitude evolution (Fig. 12a) of an arbitrary reference point situated at present on the India/Lhasa main boundary, at {29°N/86°E} as predicted by: (1) BC02 Europe APWP (blue curve), (2) the present-study East Asia APWP (red solid curve); (3) the paleolatitude inferred for Lhasa block from its $\Delta\lambda$ paleolatitude anomaly as described in section §5.2 above (red dotted curve),

and (4) the BC02 India APWP (black curve with blue confidence area), with a possible 10° northern extent of Greater India (dotted black line) as earlier suggested by Besse et al. (1984). Fig. 12b provides an elargement of Fig. 12a, with various propositions of place and date of the India collision shown as yellow stars, as proposed by older, as well as recent studies (Patzelt et al., 1996; Aitchison et al., 2007; Chen et al. 2010; Dupont-Nivet et al., 2010a; Liebke et al. 2010; Sun et al., 2010; Tan et al., 2010; Yi et al., 2011; Sun et al. 2012).

This figure leads us to address two major points. First, as a conservative hypothesis, we propose that the collision between India and Asia took place when the Lhasa paleolatitude, inferred to be 13.2° ± 8.5° south of the East Asia predicted paleolatitude prior to 50 Ma (section §5.2, Figs. 10a and 12b), and the 10° wide Greater India paleolatitude cross each other at ~55 Ma and ~8°N latitude (red star in Fig. 12b). This indirect evidence is very well corroborated by the determinations of recent paleomagnetic studies of Sun et al. (2010, 2012), Liebke et al. (2010), Chen et al. (2010), and Yi et al. (2011) (yellow stars 4 to 8, Fig. 12b). In contrast, because the predicted paleolatitude of the reference point using our new East Asia APWP (red curve) is about ~10° farther south at 50 Ma (8.9° ± 5.4°, Fig. 12b) than the paleolatitude computed after the BC02 reference APWP (blue curve), it is clear that the Aitchison et al. (2007), Tan et al. (2010) and Dupont-Nivet et al. (2010a) solutions (points 1-3, Fig. 12b) are obviously too much north of the southern boundary of Asian plate, which renders these solutions quite unsustainable.

Second, because our new East Asia APWP implies an 8.9° ± 5.4° (990 ± 600 km; Fig. 12b) position of Siberia south of its predicted paleolatitude from the BC02 Europe APWP, we propose that the total convergence between India and Siberia, through Greater India and Central Asia , is rather on the order of 18.8° ± 5.7° (2080 ± 630 km; Fig. 12b) since 50 Ma. This represents a drastic 1/3 reduction of all published previous estimates (e.g. Besse et al., 1984; Chen et al., 1993b; Patzelt et al., 1996: Dupont-Nivet, 2010a; van Hinsbergen et al., 2012, amongst other; see Table 2), which were based on the Europe reference APWP and which provide a total amount of 27.7° ± 4.3° (3070 ± 480 km; Fig. 12b) following the present analysis. We therefore conclude here that the new East Asia APWP implies significantly reduced total post-collisional intracontinental shortenings throughout Central Asia as compared to the previously proposed amounts, what should be taken into account in the whole interpretation of Asian tectonics.

6. Discussion: Causes for the 1st order Cenozoic Paleolatitude Anomaly over Asia.

We now turn to a discussion on the main causes of the Cenozoic inclination, or paleolatitude 1st-order anomaly in Asia. From our analysis, it is clear that neither systematic effects of sedimentary processes-induced inclination shallowing, nor systematic errors in age can be evoked for the very 1st-order paleolatitude anomaly we described above (section §5.1). We thus face 2 alternative causes which have already been discussed in the literature, but which still need a more thorough examination regarding the whole Asian dataset, namely: (1) a non-dipolar geomagnetic field geometry, due to either a local anomaly (e.g. Westphal, 1993; Chauvin et al., 1996) or a persistence of global non-dipolar components (e.g. a significant and long-lasting octupolar and/or quadrupolar contribution) which would have produced a large part of this anomaly (pros: Si and Van der Voo, 2001; Torsvik and Van der Voo, 2002; cons: Courtillot and Besse, 2004); (2) a tectonic cause, which we have proposed some time ago (Cogné et al., 1999), where the 1st-order paleolatitude anomaly in Asia would have been produced by some unknown and/or misunderstood relative plate movements between the western and eastern parts of Eurasia during the Mesozoic and the Cenozoic.

6.1. A geomagnetic cause.

Westphal (1993) and Chauvin et al. (1996) first suggested a possibly global or regional anomaly of the dipolar geomagnetic field at the scale of Eurasia, but did not provide any explanation as for the mechanisms. More recently, Si and Van der Voo (2001), Torsvik and Van der Voo (2002), or Dupont-Nivet et al. (2010b) advanced the main suggestions of a magnetic field anomaly. These authors suggested that some Cenozoic permanent and global, non-dipolar components, mainly octupolar, could produce the paleomagnetic inclination shallowing (between observed and expected inclinations) in middle latitudes such as in Central Asia at those times. Based on low inclinations in Central Asia, Si and Van der Voo (2001) proposed that a significant axial octupolar component g_3^0 could have persisted in the Cenozoic, at least in the ~80-20 Ma period. In order to compensate for anomaly amplitude, they proposed that this contribution of g_3^0 to geocentric axial dipole g_1^0 could have been as high as 10-15% (G3 = g_3^0/g_1^0 = 0.10 to 0.15), with no significant contribution of an axial quadrupole g_2^0 (i.e. G2 = g_2^0/g_1^0 = 0). Obviously, such high values can actually be evoked as a possible mechanism for the ~10°-12° offset of our East Asia APWP, with respect to Europe APWP (Fig. 6), which we defined as the 1st-order anomaly in §5.1 above.

In order to test for the effect of such a non-dipolar geometry on the 2nd-order anomaly due to relative tectonic movements of Asian blocks, we have tested these values. To this purpose, we have re-computed $\Delta\lambda$ paleolatitude anomaly maps for the 0-50Ma period (n=128

data), using the Europe reference APWP, after a recalculation of the quadrupole and octupole-corrected paleocolatitudes (θ) from the observed paleomagnetic inclination (I) at each locality, after the formula derived from Livermore et al. (1983) and Merrill et al. (1998):

$$\tan I = \frac{2\cos\theta + (4.5\cos^2\theta - 1.5) \times G2 + (10\cos^3\theta - 6\cos\theta) \times G3}{\sin\theta + (3\cos\theta\sin\theta) \times G2 + (7.5\cos^2\theta\sin\theta - 1.5\sin\theta) \times G3}$$

with $G2 = g_2^0/g_1^0$ and $G3 = g_3^0/g_1^0$.

These maps (Fig. 13) are to be compared with the one we computed under the dipolar geomagnetic field hypothesis (Fig.9). We propose 2 models: because of the path described by our new East Asia APWP (Fig. 6), which displays a maximum offset with respect to Europe APWP for ages older than ~30Ma, intermediate offset in the ~10-30Ma period, and a negligible discrepancy between 0 and 10 Ma, we have used variable values of G3 in constructing maps of Fig. 13a and 13b: a maximum value $G3_{max}$ for 30-50 Ma-old data ($G3_{max}$ = 0.10 in Fig. 13a; $G3_{max}$ = 0.15 in Fig. 13b), half this value for 10-30 Ma-old data (0.050 and 0.075, respectively), and G3 = 0 for 0-10 Ma-old data. Obviously, a 10% maximum g_3^0 contribution (Fig. 13a) is not high enough to compensate for the 1st-order anomaly of eastern Asian regions, where negative (-5 to -10°) $\Delta\lambda$ anomalies are still distributed over the area. We also underline that the amplitude of the negative $\Delta\lambda$ 2nd-order anomaly over Tibet and Central Asia is still very large, larger than -20° over wide areas. This figure tends to improve when modelling a 15% maximum g_3^0 contribution (Fig. 13b): the near-zero $\Delta\lambda$ anomaly area is wider over eastern Asia, and negative anomaly of Tibet and Central Asia is reduced to a more consistent ~15° magnitude. The map here obtained compares well with the one we obtained in the dipolar hypothesis using the East Asia APWP as a reference (Fig. 9b).

Indeed, analysis of these maps is not discriminatory enough to put forward a magnetic field model rather than another one but it allows to reinforce the important conclusion we reached above (§5.1): what could be the cause and origin of the 1st-order part of the $\Delta\lambda$ anomaly over Asia, geomagnetic as just discussed or tectonic as we will discuss below (§6.2), the 2nd-order anomaly, mainly distributed over the mobile blocks (Tibet, Central Asia, Indochina..) is indeed strictly originated and dominated by Cenozoic active tectonics in Asia. We also stress that even with large octupolar contributions, as large as 15% (Fig. 13b), the amplitude of this anomaly remains high, larger than 15° in some places over Tibet and Central

Asia. In contrast, the implicitly "dipolar and tectonics" map based on the East Asia APWP (Fig. 9b) tends to reduce this amplitude to a more conceivable maximum of ~10-15°.

Finally we underline that, based on the worldwide 0-200 Ma paleomagnetic database, Courtillot and Besse (2004) have presented an analysis of paleopole mean positions in 20 Ma windows, recalculated in a common-site longitude, and splitted into 3 site latitude bands: northern mid-latitude sites (25°N to 70°N), equatorial sites (25°S to 25°N) and southern mid-latitude (25°S to 70°S) sites respectively. Searching for the distinctive antisymmetrical pattern expected for a dipole and an octupole, these authors concluded that they "find no robust evidence for an octupole and estimate that values on the order of 5% are unlikely to have been exceeded in the last 200Ma". They concluded that the 200 Ma overall mean field likely reveals a significant 3 ± 2% g_2^0 quadrupole contribution in the total field and an insignificant 3 ± 8% g_3^0 octupole contribution. From this analysis, there are no clear arguments to reject the non-dipolar field hypothesis, but we now turn to the examination of the last possible cause for this very 1st-order anomaly, tectonics.

6.2. A Tectonic cause.

6.2.1. Farther south paleoposition of Siberia and East Asia by the Cenozoic.

More than a decade ago we proposed that inclination, or paleolatitude anomaly, not only in Central but overall Asia, was partly but significantly resulting from poorly known and/or misunderstood tectonic interactions between western and eastern extreme parts of Eurasia (Cogné et al., 1999). At that time, we suggested that in the frame of a dipolar magnetic field geometry, and the lack of other dominant effects such as sedimentary processes-induced paleomagnetic inclination shallowing, or systematic paleomagnetic age errors, a major cause for the Meso-Cenozoic Asian anomaly might be due to an erroneous estimate of the Siberia paleolatitude position, as predicted by the BC02 Europe APWP reference poles (actually, at that time by the Europe APWP of Besse and Courtillot, 1991, (BC91) which, to this point of view was not drastically different from BC02), and that paleomagnetic results should be considered at face values. In that hypothesis, we suggested that the Siberia south margin could have actually been located ~10° farther south of its predicted paleolatitude from the BC91 (and afterwards from BC02) reference APWP, during a significant part of the Cenozoic. This, indeed, must imply relative tectonic movements between the western (Europe) and eastern (Siberia) parts of Eurasia plate by the Cenozoic. We thus now turn to comment this tectonic interpretation, which has found significant

arguments from recent geophysical, geological and field studies. All following analysis and comments are based on 6 paleogeographic reconstructions from 90 Ma, the late Cretaceous, to Present-day (Fig. 16). These reconstructions are indeed based on a dipolar field assumption.

Overall, a first remark must be made: in all the Meso-Cenozoic reconstructions we give here (Fig. 14), the relative paleopositions and inter-relationships between the main continental parts of plates (Australia, India, Africa, Europe and North America) are strongly and quite confidently controlled not only by paleomagnetic data and synthetic APWP determinations (Besse and Courtillot, 1991, 2002), but also by inter-plates kinematics deduced from ocean floor magnetic anomalies (Müller et al., 1997, 2008) from the Atlantic to the Indian Oceans, through consistent plate circuits. The only "uncontrolled" plate position in this system is eastern Eurasia, comprising Siberia, China, and eastern Asian blocks and terranes, since they are entirely bounded by the Tethys subduction(s) to the south (e.g. Ricou, 1994, 1996), and the paleo-Pacific subduction to the east (blue lines in Fig. 14). Thus, Asia has a unique situation because up to now, these eastern Eurasian plate paleopositions only relied on the hypothesis of a rigidity between the western Eurasia parts (Europe) and the eastern Eurasia parts (Siberia and China, etc..). In our reconstructions (Fig. 14) we therefore introduce a new constraint: the paleomagnetically determined paleolatitudes of Asian continental segments, as deduced from the paleomagnetic data in the frame of a dipolar magnetic field hypothesis. To this purpose, we computed Euler rotations between Australia, India, Siberia, and all mobile Asian blocks/terranes with respect to a reference frame where Western Europe was kept fixed. The rotations where computed from (1) oceanic isochrons of Müller et al. (2008) which allow to compute the plate circuit between Europe and India, and (2) using our new East-Asia APWP to constrain Siberia and the mobile Asian blocks/terranes relative to West Europe on the one hand, and the India plate on the other hand (Table A6 in *online supplementary material*) .

6.2.2. Plate tectonics examinations and implications.

In the late Cretaceous (90Ma, Fig. 14a), with the exception of India, all parts of the Asian mosaic are already assembled, after the closure of the Mongol-Okhotsk ocean in the early Cretaceous (Kravchinsky et al., 2002; Cogné et al., 2005; Metelkin et al., 2007, 2010). The paleolatitudes of Siberia, Amuria, North and South China blocks are consistent with the predicted paleolatitude of western Eurasia (e.g. Fig. 4 and 5), following the BC02 Europe APWP. We note that possible latitudinal extensional relative movements between the western and eastern parts of Eurasia might exist at that time (red arrows in Fig. 14a), as suggested by

NE-SW and NW-SE extensions along the Tornquist-Tesseyre line (TTL in Fig. 14a, b and c), described by Bergerat et al. (2007) in their microtectonics studies of the Mesozoic structures from this area. Such an extensional context is also consistent with either the final development of the Jurassic peneplain in the Urals, which was possibly followed by a period of burial before the final cooling/exhumation from approximately the middle Cretaceous onwards (Seward et al., 1997), or the Cretaceous to Paleocene subsidence of the West Siberian basin (Rudkevich, 1976).

In the late Paleocene (60 Ma, Fig. 14b), the BC02 APWP implies that Europe has begun to slightly rotate counterclockwise (white curved arrow on Europe in Fig. 14b). Should the eastern Eurasia (Siberia, China, mobile Asian terranes, etc..) be rigidly attached to Europe, this slight rotation would have produced, owing to a long level-arm effect, a northward drift of north Siberia, as underlined by the grey sector and white arrow traced over central Europe and Siberia in Fig.14b. As a consequence, the Siberia northern parts should have been located as drawn in bold black contours with white background in Fig. 14. This drift should have been as large as ~10°-12° (up to ~1300 km) at 50-40 Ma (Fig. 14 c and d), which totally disagrees with the paleomagnetically determined paleolatitudes from Siberia, Amuria, Korea, NCB and SCB as analyzed above. Thus, in the frame of a dipolar magnetic field hypothesis, the only solution is to fix the Asian system paleolatitude in its paleomagnetically determined paleoposition (brown yellow contours in Fig. 14b, and ongoing ones). This hypothesis indeed imposes relative tectonic movements between Europe and Asia in the Cenozoic. This is in line with the microtectonics studies of Bergerat et al. (2007) in the Tornquist zone in Meso-Cenozoic times. We finally note that, at that time, the microtectonics studies on the Tornquist Tesseyre line (Bergerat et al., 2007) reveal an inversion of stress directions, the so-called Laramide inversion (dated in Danian times, ~65 Ma), where slickenside lineations (or striae) and sense of movement indicate a shift to a NE-SW compressional regime, well consistent with our paleomagnetically-based reconstructions in ongoing times.

At 50 Ma (Fig. 14c) the India plate is colliding with Asia, most probably at ~55 Ma as initially proposed by Besse et al. (1984), Patriat and Achache (1984), Patzelt et al. (1996), or more recently Huang et al. (2010) amongst others, and re-discussed above (§5.4). The intracontinental shortening has yet begun in Central Asia. It should be noticed here that accounting for paleomagnetic constraints, the southern margin of Siberia (including Amuria, e.g. see high quality paleomagnetic results of Hankard et al., 2007a) is confidently situated about 10° south of the position predicted by the BC02 reference APWP of Europe (bold black contour with white background in Figs. 14a to e). We stress here that accounting for the

differences between the predicted and observed paleolatitudes of the Tibet blocks, and especially Lhasa (e.g. Fig. 10a) with respect to Siberia, the collision took place no later than ~60 to 50 Ma, as usually admitted and recently re-assessed by Huang et al. (2010), and certainly not at ~35Ma as proposed by Aitchison et al. (2007). That late collision hypothesis is even more unsustainable in our later reconstruction at 40 Ma (Fig. 14d), where we suggest that a significant north-south intracontinental shortening between India and Siberia has already largely begun, as also recently re-assessed by Copley et al. (2010).

As in the above analysis (section §5), we would like to stress that the Central Asia deformation since 50 Ma is consistent with previous analyses and models (e.g. Tapponnier and Molnar, 1979; Tapponnier et al., 1982; Tapponnier et al., 1986; Enkin et al., 1992; Chen et al., 1993b; Halim et al., 1998a; Cogné et al., 1999), where the India-Siberia convergence is achieved by (i) an intracontinental shortening in major mountain chains (mainly Himalaya, Kunlun, Tien Shan, Qilian Shan and Altay), and (ii) a lateral escape of rigid blocks such as Indochina towards the south (Yang and Besse, 1993), or Amuria, and attached blocks (NCB, KOR, SCB) towards the east (Halim et al., 1998a; Cogné et al., 2005) along demonstrated (for Indochina Peninsula) or suspected (for East Asia) major crustal strike-slip faults (Figs. 14c to f).

Concurrently, in the west of Eurasian system, a convergence between Europe and Asia has also begun. As in Cogné et al. (1999), we propose that this convergence could be mainly absorbed within two discrete major zones (Fig. 14c): the Tornquist Tesseyre line (TTL; Fig. 14c) in Europe, and along a reactivation of the old late Paleozoic collision Ural mountain chain (UM; Fig. 14c) which separates eastern parts from western parts of Eurasia. By that time, the eastern and western parts are already converging, as demonstrated by the field and microtectonics studies of Bergerat et al. (2007), where a NE-SW convergence across TTL is proposed (red arrows in Figs. 14d and e). Due to the relative azimuths of the TTL and the convergence directions, some right-lateral strike-slip faults also develop along the TTL (black right-lateral shear arrows in Figs. 14d and e) as observed by Kopp (1999, 2007) and Bergerat et al. (2007). This NE-SW convergence across the TTL appears to be fully consistent with our inferred intraplate E-W convergence of the eastern and western ends of Eurasia, based on Cenozoic paleomagnetic reconstructions, and the eastern Asia south paleolatitudes and/or shallow magnetizations.

In our earlier hypothesis (Cogné et al., 1999), we also proposed that a significant part of this convergence could likely be achieved through Cenozoic tectonics in the Paleozoic collision Ural mountain chain. Since then, geological and structural geology studies have been

held in the southern Urals (Kopp, 2005; Verzhbitskii and Kopp, 2004, 2005) and in the northern Urals (Kopp, 2007) which appear in complete agreement with this prediction. Although the situation is somewhat complicated by Miocene times, due to the Arabian collision in the south (e.g. Verzhbitskii and Kopp, 2004), the present-day topography of the Urals unambiguously results from a Cenozoic E-W transpressive convergence between the Central Kazakhstan block and the East European craton (Puchkov, 1997; Verzhbitskii and Kopp, 2005; red arrows in Fig. 14d and e). Here also, because of the respective azimuths of convergence direction and chain orientation, a significant non-coaxial left-lateral strike-slip faulting is observed all along the chain (Puchkov, 1997; Kopp, 2005, 2007; black left-lateral shear arrows in Fig. 14 d and e). The Cenozoic, possibly mid-Eocene (Kopp, 2007; e.g. Fig. 14d) to present-day convergence across the Urals is probably much more important than across the Tornquist zone, as underlined by the fairly high present-day Urals topography which might result from the underthrusting of the thin and heavy west Siberia crust beneath the thick buoyant eastern margin of East European Platform (Kopp, 2007).

Indeed, it is difficult to estimate the exact amount of intracontinental E-W shortening across Eurasia implied either by our reconstructions (Figs. 14c to f), or by structural geology. From the reconstructions we propose in Fig. 14, a total trans-Eurasia E-W convergence ranging from 1.5° to 2° (~160 to 220 km) appears to be a reasonable value, albeit not yet geologically tested. In the same way, the shear amounts in TTL and Urals are small, probably a few km in the TTL and a few tens of km in the Urals, well below the resolution of our reconstructions.

Finally, it should be noticed that we have still not deciphered some details in these highly schematic reconstructions, such as the tectonics of the southern tethyan terranes (grey strips above Afghanistan, Iran, Turkey terranes in Fig. 14), and the transition between the Urals and the Arabia plate collision zone.

6.2.3 Arctic constraints.

A final key-point, not tackled in our previous model (Cogné et al., 1999) can now be more precisely depicted: the consistency of the northern parts of our suggested reconstructions with the Arctic Sea and the northern Alaska structures and their Cenozoic evolution. The Arctic Ocean seafloor can be schematically divided into 3 main bathymetric areas (see toponymy in Fig. A of Annex 07, in *online supplementary material*; after Jakobsson et al., 2008): (1) a large continental shelf extends offshore Europe, Russia and Siberia, comprising the north of Svalbard, the Franz Josef Land, Severnaya Zemlya, the New

Siberian and Wrangel Islands; (2) in contrast, the North America continent, north of Canada and Alaska, is bordered by an oceanic crust basin, the Canada basin, which formed between the late Jurassic and the early Cretaceous (e.g., Lawver et al., 2002; Golonka et al., 2003; Brozena et al., 2003; Glebovsky et al., 2006; Müller et al., 2008; Alvey et al., 2008; Sokolov, 2009) where, after these authors, the oceanic accretion vanished between 120 and 140 Ma; and (3) an Eurasian basin (Glebovsky et al., 2006; Alvey et al., 2008) with a somewhat complicated setting, north of Greenland.

The active Gakkel Ridge (Fig. A), extending from NE Greenland to Siberia in the southeast, is the place of the present-day Arctic accretion (e.g. Brozena et al., 2003; Glebovsky et al., 2006; Müller et al., 2008), controlling the formation of oceanic crust in the Arctic. It is connected to the Reykjanes Ridge of North Atlantic ocean, south of Iceland, through the ridge/transform system of Knippovich Ridge (toponymy from Sokolov, 2009; Fig. A). The Gakkel Ridge is separated from the now-vanished accretion center of Alpha and Mendeleev Ridges by the topographically high Lomonosov Ridge, suspected to be of continental origin (e.g. Sokolov, 2009). Opening of the Eurasian basin appears to begin around 70 Ma along the short-lived Alpha Ridge, in connection with the first stages of North Atlantic opening which separates Greenland from North America along the Run Ridge in the Labrador Sea (Fig. A). As soon as ~53 Ma (anomaly 24), the oceanic crust accretion center tends to move to the Gakkel Ridge. Then follows a period of unstable spreading between these 2 centers, between 53 and ~40 Ma, when the Alpha Ridge stops functioning (e.g. Glebovsy et al., 2006). Since then, the Arctic basin continuously spreads, at very low spreading rates of ~10 mm/yr (total rates; Brozena et al., 2003; Glebovsky et al., 2006) along the Gakkel Ridge, connected to the North Atlantic Reykjanes Ridge by the Knippovich ridge/transform system.

Our models of Fig.14 include a rough sketch of this Cenozoic evolution of the Arctic Ocean. At 60 Ma, the Eurasian basin has begun opening along the Alpha Ridge (AR in Fig. 14b), and Greenland is shifting apart from North America along the Run Ridge (RR, Fig. 14b), whereas relative converging movements between Europe and Siberia is initiated, as detailed in section §6.2.2 above. At 50 Ma, the accretion is unstable in the Arctic (Glebovsky et al., 2006), and probably jointly acts on the Alpha and Gakkel Ridges, shown as dotted lines divergent centers in Fig. 14c. This kinematics scheme appears consistent with our inferred stability in latitude of Central Eurasia and East Asia/Siberia in the Cenozoic. At 40 Ma, the Alpha Ridge has vanished, and all the Arctic oceanic crust accretion has now shifted along the Gakkel Ridge, on the other side of the Lomonosov Ridge (Fig. 14d, Fig. A). More to the

south, the Run Ridge vanished, and the accretion center of the northern Atlantic ocean migrated from the west to the east of Greenland, along the Knippovich Ridge (Fig. 14d, Fig. A), itself connected to the Reykjannes Ridge to the south.

Final arguments lend support to this model when examining the northward general convergence of East Siberia with North America, starting from ~50-30 Ma (e.g. Hankard et al., 2007a; red curved arrows in Figs. 14d and e), ending by the Present-day geometry (Fig. 14f). This convergence appears to be oblique between the Chukotka subplate (Golonka et al., 2003; Fig. A) and the Arctic Alaska (Figs. 14d and e; Fig. A), fully consistent with (1) the Cenozoic to Present transpressive right-lateral shear movements in the Arctic Alaska, allowing rise of the Brooks Range (Fig. A) and dextral ~E-W shear zone developments within this range (e.g. Wirth et al., 2002; Golonka et al., 2003), and (2) the Cenozoic transpressive deformation along the Moma rift system (e.g. Gaina et al., 2002). Here again, the plate tectonics and intracontinental deformation history we propose in Fig. 14, based on a latitudinal stability of eastern Eurasia through Cenozoic times deduced from the analysis of paleomagnetic Inclination Anomaly in China and Central Asia, is verified by field observations in those very remote northern across-the-pole regions.

This brief description of northern Arctic kinematics not only supports our Cenozoic reconstructions, but also reinforces our idea of a decoupling between eastern and western Eurasia by those times. Overall, we thus conclude that the Central Asia paleomagnetic 1st-order "Inclination Anomaly" or "Paleolatitude Anomaly" might solely be supported by demonstrated geophysical and geological data and their interpretations from East Europe, Central Russia and northern Arctic regions, up to Alaska, in the frame of a global dipolar magnetic field geometry in the Cenozoic, without any need to invoke sedimentary flattening effects of magnetization in Asian localities, or non-dipolar, mainly octupolar, magnetic field geometry.

7. Summary and conclusions.

(1) Whether it be of tectonic and/or geomagnetic origin, the Paleolatitude "Anomaly" is observed all over the Asian continent, from the Asian Middle-East to the eastern Chinese blocks. The consistency of paleomagnetic directions over the Siberian Craton, Amuria, North and South China Blocks, and the Korean peninsula permits the use of these blocks for the construction of a new 130-0 Ma reference Apparent Polar Wandering Path (APWP) for East Asia, distinct from the currently used European APWP. This new APWP is the only one capable of deciphering late Mesozoic and Cenozoic deformation East of the Urals.

(2) Comparison and consistency of data from sedimentary (mainly redbeds) formations and igneous (mainly effusive) formations show that flattening of paleomagnetic inclination due to some sedimentary processes in redbeds is present, but it is not the dominant mechanism responsible for this anomaly observed all over Asia. We demonstrate this to be especially true for stable blocks from which our new East Asia APWP has been defined. We suggest it is also valid in smaller mobile blocks, where data collection allows comparison (e.g. Lhasa block, Indochina blocks…). Finally, age uncertainties inherents to redbeds may be invoked in some cases, inducing an apparently strong inclination shallowing effect (e.g. Miocene formations from Qaidam).

(3) A comparison of paleolatitude differences between observed and expected paleolatitudes from the new reference APWP of East Asia, between mobile and stable blocks (2^{nd}-order anomaly) allows us to propose: (1) a 11.3° ± 9.2° (1250 ± 1020 km; whole Tibet) to 13.2° ± 8.5° (1450 ± 940 km; Lhasa block only) post-Cretaceous northward convergence of Tibet with Siberia which is significantly lower than previous estimates of 1700 ± 610 km of Chen et al. (1993b); (2) a 4.3° ± 6.6° (480 ± 730 km) of Cenozoic southward divergence of Indochina with respect to Siberia. Compared to Siberia, this appears rather insignificant but compared to Lhasa block of Tibet this results in a total N-S post-Cretaceous divergence of 17.5° ± 8.6° (1950 ± 950 km). This is in line with previous estimates of 6.8° ± 2.8° (750 ± 310 km) of southward extrusion of Indochina with respect to South China proposed by Yang and Besse (1993) for the Khorat Plateau, and underlines the large amounts of relative movements between mobile blocks of Asia in the Cenozoic. Northward post-Cretaceous convergence of Qaidam (11.9° ± 8.0° or 1320 ± 890 km) and Tarim/Jungar blocks (9.7° ± 5.5° or 1080 ± 610 km) with Siberia are not inconsistent with previous results, although they might be somewhat overestimated. We acknowledge that more than 90% of the results from these blocks come from redbeds and caution that the above estimates could be biased by a few degrees (up to ~5° ?) due to local sediment related inclination shallowing (e.g. Dupont-Nivet et al., 2010).

(4) The newly compiled East Asia APWP also has consequences on the interpreted timing and latitudinal location of India collision and the total amount of intracontinental shortening between India and Siberia and Tibet, respectively. It reinforces the first evaluation of a collision age around 55 Ma, as proposed by Patriat and Achache (1984), and supports a collision location at 5°-10° N latitude. This is not really new, but it is worth emphasizing since recent publications have reopenened the debate (e.g. Aitchison et al., 2007; Tan et al., 2010; Dupont-Nivet et al., 2010a). The consequences on the total amount of intracontinental

shortening is of greater importance. The East Asian APWP presented herein predicts an ~33% reduction of the total amount of post-collisional intracontinental convergence between India and Siberia. The estimate of 27.7° ± 4.3° (3070 ± 480 km) rendered when using BC02 Europe APWP is reduced to 18.8° ± 5.7° (2080 ± 630 km). Consequently, interpretations and evaluations of Asian tectonics based on previous APWP should fall into questions.

(5) From our analysis of the anomaly, and excluding inclination flattening as a dominant cause all over Asia, we suggest that two main mechanisms might be responsible for these shallow magnetization: (1) a long-lasting magnetic field anomaly, as poposed by Westphal (1993), Chauvin et al. (1996), Si and Van der Voo (2001), or Dupont-Nivet et al. (2010b), and/or (2) a poorly understood paleoposition of Siberia and Asian blocks which has consequences on Eurasia tectonics. In line with Si and Van der Voo (2001), we notice that introducing an axial-octupolar contribution in computation of paleopoles reduce this anomaly. However, a large contribution of G3, as large as 15%, is required in order to obtain a significant reduction of the anomaly in the eastern Asian regions. From a 200-0 Ma worldwide dataset, Courtillot and Besse (2004) concluded that a G3 contribution is probably insignificant. Therefore, if significant and long-lasting non-dipolar components contributions in the magnetic field are to be the origin of Cenozoic Inclination Anomaly, it is still far from being firmly demonstrated.

(6) Turning back to the reassuring and generally admitted hypothesis of a mean dipolar magnetic field geometry, our analysis pleads to an ill-understood plate tectonic evolution of Eurasia in the Cenozoic. At face value, paleolatitude of Siberia and East Asia regions appear to be ~10° lower than expected from BC02 APWP in the Cenozoic, whereas this APWP depicts a consistent relative slight counterclockwise rotation of Europe. This situation inevitably results in relative tectonic movements between Europe and Siberia, thus a continental deformation Eurasia as a whole. We proposed this scheme more than a decade ago (Cogné et al., 1999), and at that time, very few publications were available to lend support to this idea. Since then, a number of field studies have been published (e.g. Puchkov, 1997; Bergerat et al., 2007; Kopp, 1999, 2005, 2007; Verzhbitskii and Kopp, 2004, 2005) which all describe structures in accordance with our predicted Cenozoic tectonic movements across Eurasia. We propose that relative movements between Europe and Siberia are mainly located along 2 discrete tectonic zones, the Tornquist-Tesseyre Line in Europe and the Ural mountain chain separating Russia from Siberia. The Tornquist-Tesseyre Line is probably less active than the Urals and reveals Cenozoic transpressive dextral convergence between central and western Europe while important transpressive sinistral relative shortening is acting along the

Urals. These tectonic movements, both in type and sense, are fully consistent with our predicted kinematics. However, the exact amount of convergence across Eurasia implied by our model is difficult to evaluate precisely, but we suggest that a total of 1.5° to 2° (160-220 km) seems reasonable and sufficient.

(7) The compatibility of our model has been tested in Arctic regions, owing to recent compilations and publications of Arctic Ocean geophysical and tectonics studies (e.g., Golonka et al., 2003; Brozena et al., 2003; Glebovsky et al., 2006; Müller et al., 2008; Sokolov, 2009). We demonstrate the compatibility of our model with Cenozoic Arctic Ocean opening along the Gakkel Ridge, and also the consistency between inferred Siberia-Alaska convergence with transpressive right-lateral tectonics of the Brooks Range in Arctic Alaska (e.g. Wirth et al., 2002; Golonka et al., 2003).

(8) Lastly, a thorough examination of the Asian paleomagnetic database, and a detailed analysis of Tertiary Inclination, or Paleolatitude Anomaly leads to both a confirmation and a reappraisal of Central Asia kinematics and tectonic movements in response to the India collision. Following the dipolar magnetic field hypothesis, we propose a kinematic model for Cenozoic deformation of whole Eurasia. This model predicts relative movements on at least 3 major tectonic boundaries, Tornquist-Tesseyre zone, Urals Mountains, and Arctic Ocean, as far as northern Alaska. These predicted movements have been consistently described by regional studies. This predictability is indeed one of the strongests argument in favor of a predominantly tectonic origin of Central Asia Inclination Anomaly.

Acknowledgements.

M. Bazhenov, R. Enkin, B. Huang, C. Langereis, D. van Hinsbergen and X. Zhao have provided constructive and helpful comments and criticisms on previous versions of this paper. This is contribution XXXX of IPGP and Sorbonne Paris Cité.

List of 7 files in online supplementary material.

Table A1: Mesozoic and Cenozoic selected paleomagnetic poles of Asia, as sorted from a compilation of Global Paleomagnetic Database 2004 and 2005-2008 literature following Thomson ISI web of sciences reference system (N=533), and reference list.

Table A2: Synthesis of the total number of 0-175 Ma selected data.

Table A3: Number of 0-140 Ma data used in construction of anomaly maps (Fig.3, 9 and 13).

Table A4: Distribution of 0-140 Ma rocktypes used in construction of anomaly maps (Fig.3, 9 and 13).

Table A5: Number of 0-140 Ma data used in East Asia APWP construction.

Table A6: Euler poles of finite rotations of various blocks / terranes shown in Fig. 14, in a fixed West Europe reference frame

Figure A: International Bathymetric Chart of the Arctic Ocean (IBCAO) of Jakobsson et al. (2008) with toponymy, as cited in text. Topographic heights are given in the bar scale.

References.

Achache, J., Courtillot, V., and Zhou, Y.X., Paleomagnetic and tectonic evolution of South Tibet since Middle Cretaceous times: new paleomagnetic data and synthesis, *J. Geophys. Res., 89*, 10311-10339, 1984.

Aitchison, J.C., Ali, J.R., and Davis, A.M., When and where did India and Asia Collide?, *J. Geophys. Res., 112,* B054203, doi: 10.1029/2006JB004706, 2007.

Ali, J.R., and Aitchison, J.C., Greater India, *Earth Sci. Rev., 72*, 169-188, 2005.

Alvey, A, Gaina, C., Kuznir, N.J., and Torsvik, T.H., Integrated crustal thickness mapping and plate reconstructions for the high Arctic, *Earth Planet. Sci. Lett., 274*, 310-321, 2008.

Avouac, J.P., Tapponnier, P., Bai, M., Wang, G., and You, H., Active faulting and folding in the northern Tien Shan (Xinjiang, China), *J. Geophys. Res., 98,* 6755-6804, 1993.

Bazhenov, M. L., and A. V. Mikolaichuk, Paleomagnetism of Paleogene basalts from the Tien Shan, Kyrgyzstan: Rigid Eurasia and dipole geomagnetic field, *Earth Planet. Sci. Lett., 195*, 155 – 166, 2002.

Bergerat, F., Angelier, J., and Andreasson P.R., Evolution of paleostress field and brittle deformation of the Tornquist Zone in Scania (Sweden) during Permo-Mesozoic and Cenozoic times, Tectonophysics, 444, 93-110, 2007.

Besse, J., and V. Courtillot, Revised and synthetic apparent polar wander paths of the African, Eurasian, North American, and Indian plates and true polar wander since 200 Ma, *J. Geophys. Res., 96,* 4029- 4050, 1991.

Besse, J. and V. Courtillot, Apparent and true polar wander and the geometry of the geomagnetic field over the last 200 Myr, *J. Geophys. Res., 107,* 1-31, 2002.

Besse, J., Courtillot, V., Pozzi, J.P., Westphal, M. and Zhou, Y., 1984. Palaeomagnetic estimates of crustal shortening in the Himalayan thrusts and Zangpo suture, *Nature, 311*, 621-626, 1984.

Brozena, J.M., Childers, V.A., Lawyer, L.A., Gahagan, L.M., Forsberg, R., Faleide, J.I., and Eldholm, O, New aerogeophysical study of the Eurasia Basin and Lomonosov Ridge: implications for basin development, *Geology, 31*, 9, 825-828, 2003.

Chauvin, A., Perroud, H., and Bazhenov, M.L., Anomalous low paleomagnetic inclinations from Oligocene-lower Miocene red beds of south-west Tien Shan, central Asia, *Geophys. J. Int., 126*, 303- 313, 1996.

Chen, J.S., Huang, B.C., and Sun, L., New constraints on the India-Asia collision: Paleomagnetic reconnaissance on the Linzizong Group in the Lhasa Block, China, *Tectonophysics, 489*, 189-209, 2010.

Chen, Y., Cogné, J.P., and V. Courtillot, V., New Cretaceous paleomagnetic poles from the Tarim Basin, northwestern China, *Earth Planet. Sci. Lett., 114,* 17– 38, 1992.

Chen,Y., Cogné, J.P., Courtillot, V., Tapponnier, P., Zhu, X.Y., Cretaceous paleomagnetic results from western Tibet and tectonic implications, *J. Geophys. Res., 98*, 17981-17999, 1993a.

Chen, Y., Courtillot, V., Cogné, J.P., Besse, J., Yang, Z.H., and Enkin, R.J., The configuration of Asia prior to the collision of India: Cretaceous paleomagnetic constraints*, J. Geophys. Res., 98*, 21927-21941, 1993b.

Coe, R.S., B.R. Globerman, P.W. Plumley, and G.A. Thrupp, Paleomagnetic results from Alaska and their tectonic implications, in *Tectonostratigraphic Terranes of the Circum-Pacific Region*, edited by D.G. Howell, pp. 85-108, Circum-Pac. Counc. for Energy and Miner. Resour., Houston, Tex., 1985

Cogné, J.P., PaleoMac: a Macintosh™ application for treating paleomagnetic data and making plate reconstructions, *Geochem.Geophys.Geosyst., 4, 1,* doi:10.1029/2001GC000227, 2003.

Cogné, J.P., Chen, Y., Courtillot, V., Rocher, F., Wang, G., Bai, M., and You, H., A paleomagnetic study of Mesozoic sediments from the Junggar and Turfan basins, northwestem China, *Earth Planet. Sci. Lett., 133*, 353-366, 1995.

Cogné, J.P., Halim, N., Chen, Y., Courtillot, V., Resolving the problem of shallow magnetizations of Tertiary age in Central Asia: insights from paleomagnetic data from the Qiangtang, Kunlun and Qaidam blocks (Tibet, China), and a new hypothesis, *J. Geophys. Res., 104*, 17715-17734, 1999.

Cogné, J. P., V. Kravchinsky, N. Halim, and F. Hankard, Late Jurassic-Early Cretaceous closure of the Mongol-Okhotsk Ocean demonstrated by new Mesozoic paleomagnetic results from the Trans-Baïkal area (SE Siberia), *Geophys. J. Int., 163*, 813- 832, 2005.

Copley, A., J. P. Avouac, and J. Y. Royer, The India-Asia collision and the Cenozoic slowdown of the Indian

plate: Implications for the forces driving plate motions, *Journal of Geophysical Research*, *115*, B03410, doi:10.1029/2009JB006634, 2010.

Courtillot, V. and Besse, J., A long-term octupolar component in the geomagnetic field? (0-200 million years B.P.), in: *Timescales of the Paleomagnetic Field*, Channell, J.E.T., Kent, D.V., and Meert, J.G. Eds., *Geophys. Monogr. Ser, A.G.U., 145*, 59-74, 2004.

Dewey, J.F., Shackleton R.M., Chang, C.F. and Sun, Y.Y., The Tectonic Evolution of the Tibetan Plateau, *Trans. R. Soc. London, Ser. A*, 327, 1594, 379-413, doi: 10.1098/rsta.1988.0135, 1988

Dupont-Nivet, G., Butler, R.F., Paleomagnetism indicates no Neogene vertical axis rotations of the northeastern Tibetan Plateau, *J. Geophys. Res., 108*, 2386, doi:10.1029/2003JB002399, 2003.

Dupont-Nivet, G., Guo, Z., Butler, R.F., and Jia, C., Discordant paleomagnetic direction in Miocene rocks from the central Tarim Basin: Evidence for local deformation and inclination shallowing, *Earth Planet. Sci. Lett., 199*, 473 – 482, 2002.

Dupont-Nivet, G., Lippert, P.C., van Hinsbergen, D.J.J, Meijers, M.J.M., and Kapp, P., Paleolatitude and age of the Indo-Asia collision: paleomagnetic constraints, *Geophys. J. Int., 182,* 1189-1198, doi: 10.1111/j.1365-246X.2010.04697.x, 2010a.

Dupont-Nivet, G., van Hinsbergen, D.J.J, and Torsvik, T.H., Persistently low Asian paleolatitudes: implications for the India-Asia collision history, *Tectonics*, *29*, TC5016, doi:10.1029/2008TC002437, 2010b.

Enkin, R., Courtillot, V., Xing, L., Zhang, Z., Zhuang, Z., and Zhang, J., The stationary Cretaceous paleomagnetic poles of Sichuan (South China Block), *Tectonics,* **10,** 547–559, 1991.

Enkin, R.J., Yang, Z., Chen, Y. & Courtillot, V., Paleomagnetic Constraints on the Geodynamic History of the Major Blocks of China From the Permian to the Present, *J. Geophys. Res., 97,* 13 953-13 989, 1992.

Fisher R. Dispersion on a sphere. *Proc. R. Soc. London, Ser.A, No.217*, 295-305, 1953.

Funahara, S., Nishiwaki, N., Miki, M., Murata, F., Otofuji, Y., Wang, Y.Z., Paleomagnetic study of Cretaceous rocks from the Yangtze block, central Yunnan, China: implications for the India-Asia collision, *Earth Planet. Sci. Letters, 113*, 77-91, 1992.

Gaina, C., Roest, W.R., and Müller, R.D., Late Cretaceous – Cenozoic deformation of northeast Asia, *Earth Planet. Sci. Lett., 197*, 273-286, 2002.

Garzanti, E., Comment on "When and where did India and Asia collide?" by J.C. Aitchison, J.R. Ali and A.M. Davis, *J. Geophys. Res., 113*, B04411, doi: 10.10292007JB005276, 2008.

Gilder, S., and Courtillot, V., Timing of the North-South China Collision from New Middle to Late Mesozoic Paleomagnetic Data from the North China Block, *J. geophys. Res., 102,* 17 713–17 727, 1997.

Gilder, S.A., Zhao, X.X., Coe, R.S.,Wu, H.R., and Kuang, G.D., 1993. Discordance of Jurassic paleomagnetic data from South China and their tectonic implications, *Earth planet. Sci. Lett., 119***,** 259–269, 1993a.

Gilder, S.A., Coe, R.S., Wu, H., Kuang, G., Zhao,X., Wu, Q., Tang, X., Cretaceous and Tertiary paleomagnetic results from Southeast China and their tectonic implications, Earth Planet. Sci. Letters, 117, 637-652, 1993b.

Gilder, S. A., X. X. Zhao, R. S. Coe, Z. F. Meng, V. Courtillot, and J. Besse, Paleomagnetism, tectonics and geology of the southern Tarim Basin, northwestern China, *J. Geophys. Res., 101*, 22,015 – 22,031, doi:10.1029/96JB01647, 1996.

Gilder, S., Y. Chen, and S. Sen, Oligo-Miocene magnetostratigraphy and rock magnetism of the Xishuigou section, Subei (Gansu Province, western China), and implications for shallow inclinations in central Asia, *J. Geophys. Res., 106,* 30,505 – 30,521, doi:10.1029/2001JB000325, 2001.

Gilder, S., Chen, Y., Cogné, J.P., Tan, X., Courtillot, V., Sun, D., Li, Y., Paleomagnetism of Upper Jurassic to Lower Cretaceous volcanic and sedimentary rocks from the western Tarim Basin and implications for inclination shallowing and absolute dating of the M-0 (ISEA?) chron, *Earth Planet. Sci. Letters, 206*, 587-600, 2003.

Gilder, S. A., Gomez, J., Chen, Y., and Cogné, J.P., A new paleogeographic configuration of the Eurasian landmass resolves a paleomagnetic paradox of the Tarim Basin (China), Tectonics, 27, TC1012, doi:10.1029/2007TC002155, 2006.

Glebovsky, V.Yu., Kaminsky, V.D., Minakov, A.N., Merkur'ev, S.A., Childers, V.A., and Brozena, J.M., Formation of the Eurasia basin in the Arctic Ocean as inferred from geohistorical analysis of the anomalous magnetic field, *Geotectonics, 40*, 4, 263-281, doi: 10.1134/S0016852106040029, 2006.

Golonka, J., Bocharova, N.Y., Ford, D., Edrich, M.E., Bednarczyk, J., and Wildharber, J., Paleogeographic reconstructions and basins development of the Arctic, *Marine Petrol. Geol., 20*, 211-248, doi: 10.1016/S0264-8172(03)00043-6, 2003.

Gradstein, F.M., Ogg, J.G., Smith, A.G., Agterberg, F.P., Bleeker, W., Cooper, R.A., Davydov, V. and Gibbard, P., A Geologic Time Scale, *Cambridge Univ. Press, U.K.,* 589 pp., doi:10.4095/215638, 2004.

Halim, N., Cogné, J.P., Chen, Y., Atasiei, R., Besse, J., Courtillot, V., Gilder, S., Marcoux, J., Zhao, R.L., New Cretaceous and early Tertiary paleomagnetic results from Xining-Lanzhou basin, Kunlun and Qiangtang blocks, China: implications on the geodynamic evolution of Asia, *J. Geophys. Res., 103*, 21025-21045, 1998a.

Halim, N., Kravchinsky, V., Gilder, S., Cogné, J.P., Alexyutin, M., Sorokin, A., and Courtillot, V., 1998b. A Paleomagnetic study from the Mongol-Okhotsk Region: Rotated Early Cretaceous Volcanics and Remagnetized Mesozoic Sediments, *Earth planet. Sci. Lett., 159,* 133–146, 1998b.

Hall, R., van Hattum, M.W.A. and W. Spakman, W., (2008), Impact of India- Asia collision on SE Asia: The record in Borneo, *Tectonophysics*, 451, 366–389, doi:10.1016/j.tecto.2007.11.058, 2008.

Hankard, F., Cogné, J.P., Kravchinsky, V.A., Carporzen, L., Bayasgalan, A., and Lkhagvadorj, P., New Tertiary paleomagnetic poles from Mongolia and Siberia at 40, 30, 20, and 13 Ma: Clues on the inclination shallowing problem in Central Asia, *J. Geophys. Res., 112*, B02101, doi:10.1029/2006JB004488, 2007a.

Hankard, F., Cogné, J.P., Quidelleur, X., Bayasgalan, A., and Lkhagvadorj, P., Paleomagnetism and K-Ar dating of Cretaceous basalts from Mongolia. *Geophys. J. Int., 169,* 898-908, doi: 10.1111/j.1365-246X.2007.03292.x, 2007b.

Hankard, F., Cogné, J.P., Lagroix, F., Quidelleur, X., Kravchinsky, V.A., Bayasgalan, A., Lkhagvadorj, P., Palaeomagnetic results from Palaeocene basalts from Mongolia reveal no inclination shallowing at 60 Ma in Central Asia*, Geophys. J. Int., 172*, 87-102, 2008.

Huang, K. & Opdyke, N.D., Paleomagnetism of Jurassic rocks from southwestern Sichuan and the timing of the closure of the Qinling suture, *Tectonophysics, 200,* 299–316, 1991.

Huang, B. C., Piper, J.D.A., Wang, Y.C., He, H.Y., and Zhu, R.X., Paleomagnetic and geochronological constraints on the post-collisional northward convergence of the southwest Tian Shan, NW China, *Tectonophysics, 409*, 107-124, 10.1016/j.tecto.2005.08.018, 2005.

Huang, B. C., Piper, J.D.A., Peng, S.T., Liu, T., Li, Z., Wang, Q.C., and Zhu, R.X., Magnetostratigraphic study of the Kuche Depression, Tarim Basin, and Cenozoic uplift of the Tian Shan Range, Western China, *Earth Planet. Sci. Lett., 251*, 346-364, doi:10.1016/j.epsl.2006.09.020, 2006.

Huang, B.C., Piper, J.D.A., Zhang, C., Li, Z., Zhu, R., Paleomagnetism of Cretaceous rocks in the Jiodong Peninsula, eastern China: Insight into block rotationsand neotectonic deformation in eastern Asia, *J. Geophys. Res., 112*, B03106, 2007.

Huang B.C., Chen, J.S. and Yi, Z.Y., Paleomagnetic discussion of when and where India and Asia initially collided, *Chinese Journal of Geophysics, 53*, 9, 2010 *(in Chinese)*.

Jaeger, J.J., Courtillot, V., and Tapponnier,P., Paleontological view of the ages of the Deccan Traps, the Cretaceous/Tertiary boundary and the India-Asia collision*, Geology, 17 (4)*, 316-319, 1989.

Jakobsson, M., Macnab, R., Mayer, L., Anderson, R., Edwards, M., Hatzky, J., Schenke, H-W., and Johnson, P., An improved bathymetric portrayal of the Arctic Ocean: Implications for ocean modeling and geological, geophysical and oceanographic analyses, Geophys. Res. Lett., 35, L07602, doi:10.1029/2008GL033520, 2008.

Jolivet, L., Tamaki, K., Fournier, M., Japan sea, opening history and mechanism: a synthesis: Northeast Japan: a case history of subduction, *J. Geophys. Res, 99*, 22237-22259, 1994.

Kopp, M.L., Transeuropean dextral shear along the Tornquist line and supposed kinematics of the East European subplate in the Cenozoic, *Theoretical and regional issues of geodynamics transactions, Moscow Nauka, 515*, 84-107, 1999 *(in Russian)*.

Kopp, M.L., Recent deformation of the southern Urals and the Mugodzhary mountains and its possible origin, *Geotectonics, 39,* 5, 364-388, 2005.

Kopp, M.L., Loz'va dislocations of the North Transural region: a response to neotectonic underthrusting of the West Siberian Platform beneath the Urals, *Doklady Earth Sciences, 417A*, 9, 1342-1347, 2007.

Kovalenko, D.V., Paleomagnetism of late Paleozoic, Mesozoic, and Cenozoic rocks in Mongolia, *Russian Geol. Geophys., 51*, 329-345, 2010.

Kravchinsky, V. A., J. P. Cogné, W. Harbert, and M. I. Kuzmin, Evolution of the Mongol-Okhotsk ocean as constrained by new paleomagnetic data from the Mongol-Okhotsk suture zone, *Geophys. J. Int., 148*, 34-57, 2002.

Lawver, L.A., Grantz, A., and Gahagan, L.M., Plate kinematic evolution of the present Arctic region since the Ordovician, *Geol. Soc. Amer. Spec. Pub., 360*, 337-362, 2002.

Lee, Y.S., Ishikawa, N., Kim, W.K., Paleomagnetism of Tertiary rocks on the Korean Peninsula: tectonic implications for the opening of the East Sea (Sea of Japan), *Tectonophysics, 304*, 131-149, 1999.

Leloup, P.H., Lacassin, R., Tapponnier, P., Scharer, U., Zhong, D.L., Liu, X.H., Zhang, L.S., Ji, S.C., and Trinh, P.T., The Ailao Shan-Red River shear zone (Yunnan, China), Tertiary transform boundary of Indochina, *Tectonophysics, 251*, 3-10, 1995.

Liebke, U., Appel, E., Ding, L., Neumann, U., Antolin, B., and Xu, Q., Position of the Lhasa terrane prior to India-Asia collision derived from paleomagnetic inclinations of 53 Ma old dykes of the Linzhou Basin: constraints on the age of collision and post-collisional shortening within the Tibetan Plateau, *Geophys. J. Int.*, doi: 10.1111/j.1365-246X.2010.04698.x, 2010.

Lin, J.-L. and Watts, D.R., Paleomagnetic results from the Tibetan plateau, *Phil. Trans. R. Soc. London, Ser. A, 327*, 239-262, 1988.

Lin, J.L., Fuller, M., and Zhang, W.Y., Preliminary Phanerozoic polar wander paths for the North and South China blocks, *Nature, 313,* 444–449, 1985.

Lippert, P.C., Zhao, X., Coe, R.S. and Lo, C.H., Palaeomagnetism and 40Ar/39Ar geochronology of upper Paleogene volcanic rocks from Central Tibet: implications for the Cenozoic inclination anomaly, the paleolatitude of Tibet and post-50 Ma shortening within Asia*, Geophys. J. Int, 184*, 131-161, 2011.

Livermore, R.A., Vine, F.J., and Smith, A.G., Plate motions and the geomagnetic field - I. Quaternary and late Tertiary, *Geophys. J. R. astron. Soc.*, 73, 153-171, 1983.

Mardia K.V., and Gadsden, R.J., A small circle of best fit for spherical data and areas of vulcanism, *Appl. Statist., 26*, 238-245, 1977.

McElhinny, M. W., and Lock, J., IAGA paleomagnetic data bases with access, *Surv. Geophys., 17*, 575-591, 1996.

Merrill, R.T., McFadden, M.W., and McFadden, P.L., *The Magnetic Field of the Earth*, Intern. Geophysics Series 63, Academic Press, London, 1998.

Métivier, F., Gaudemer, Y., Tapponnier, P., and Meyer, B., Northeastward growth of the Tibet plateau from balanced reconstruction of two depositional areas: the Qaidam and Hexi corridor basins, *Tectonics, 17*, 823-842, 1998.

Metelkin, D.V., I.V. Gordienko and V.S. Klimuk, Paleomagnetism of Upper Jurassic basalts from Transbaikalia: new data on the time of closure of the Mongol-Okhotsk Ocean and Mesozoic intraplate tectonics of Central Asia, *Russian Geol. Geophys., 48*, 825-834, 2007.

Metelkin, D.V., V.A. Vernikovsky, A. Yu. Kazansky and M.T.D. Wingate, Late Mesozoic tectonics of Central Asia based on paleomagnetic evidence, *Gondwana Res., 18*, 400-419, 2010.

Meyer, B., Tapponnier, P., Gaudemer, Y., Peltzer, G., Guo, S.M., and Chen Z., Rate of left-lateral movement along the easternmost segment of the Altyn-Tagh fault, east of 96°E (China), *Geophys. J. Int., 124*, 29-44, 1996.

Meyer, B., Tapponnier, P., Bourjot, L., Métivier, F., Gaudemer, Y., Peltzer, G., Guo, S.M., and Chen, Z., Crustal thickening in Gansu-Qinghai, lithospheric mantle subduction, and oblique, strike-slip controlled growth of the Tibet plateau, *Geophys. J. Int., 135*, 1-47, 1998.

Molnar, P. and Tapponnier, P., 1975, Cenozoic tectonics of Asia: effects of a continental collision, *Science., 189,* 419-426, 1975.

Müller, R.D., W.R. Roest, J.Y. Royer, L.M. Gahagan, J.G. Sclater, Digital isochrons of the world's ocean floor, *J. Geophys. Res.* 102, 3211-3214, 1997.

Müller, R.D., Sdrolias, M., Gaina, C., and Roest, W.R., Age, spreading rates and spreading asymmetry of the world's ocean crust, Geochem. Geophys. Geosys., 9, Q04006, doi: 10.1029/2007GC001743, 2008.

Najman, Y., Appel, E., Boudhager-Fadel, M., Bown, P., Carter, A., Garzanti, E., Godin, L., Han, J.T., Liebke, U., Oliver, G., Parrish, R. and Vezzoli, G., Timing of India-Asia collision: Geological, biostratigraphic, and paleomagnetic constraints, *J. Geophys. Res., 115*, B12416, doi: 10.1029/2010JB007673, 2010.

Otofuji, Y., Matsuda, T., Itaya, T., Shibata, T., Matsumoto, M., Yamanoto, T., Morimoto, C., Kulinich, R.G., Zimin, P.S., Matunin, A.P., Sakhno, V.G., Kimara, K., Late Cretaceous to early Paleogene paleomagnetic results from Sikhote Alin, far eastern Russia: implications for the deformation of East Asia, *Earth Planet. Sci. Letters, 130*, 95-108, 1995.

Otofuji, Y., Miura, D., Takaba, K., Takemoto, K., Narumoto, K., Zaman, H., Inokchi, H., Kulinich, R.G., Zimin, P.S., Sakhno, V., Counter-clockwise rotation of the eastern part of the Mongolia block: Early Cretaceous palaeomagnetic results from Bikin, Far Eastern Russia, *Geophys. J. Int., 164*, 15-24, 2006.

Park, Y.E., Doh, S.J., Ryu, I.C., Suk, D., A synthesis of Cretaceous palaeomagnetic data from South Korea: tectonic implications in East Asia., *Geophys. J. Int., 162*, 709-724, 2005.

Patriat, P., and Achache, J., India collision chronology has implications for crustal shortening and driving mechanism of plates, *Nature, 311*, 615-621, 1984.

Patzelt, A., Li, H., Wang, J., and Appel, E., Palaeomagnetism of Cretaceous to Tertiary sediments from southern Tibet: evidence for the extent of the northern margin of India prior to the collision with Eurasia: *Tectonophysics, 259*, 259-284, 1996.

Puchkov, V.N., Structure and geodynamics of Uralian orogen, in Burg, J.P. and Ford, M., eds, Orogeny Through Time, *Geol. Soc. Spec. Publ., 121,* 201-236, 1997.

Pei, J.L., Sun, Z.M, Wang, X.S., Zhao, Y., Ge, X.H., Guo, X.Z., Li, H.B., and Si, J.L., Evidence for Tibetan plateau uplift in Qaidam basin before Eocene-Oligocene boundary and its climatic implications, *J. Earth Sci., 20*, 430-437, doi: 10.1007/s12583-009-0035-y, 2009.

Petit, C., and Deverchère, J., Structure and evolution of the Baikal Rift: a synthesis, *Geochem. Geophys. Geosys., 7,* Q11016, doi: 10.129/2006GC001265, 2006.

Pruner, P. (1992), Paleomagnetism and paleogeography of Mongolia from the Carboniferous to Cretaceous - final report, *Phys. Earth Planet. Int.*, *70*, 169-177.

Replumaz, A., and Tapponnier, P., Reconstruction of the deformed collision zone between India and Asia by backward motion of lithospheric blocks*, J. Geophys. Res., 108, B6*, 2285, doi:10.1029/2001JB000661, 2003.

Ricou L.E., Tethys reconstructed: plates, continental fragments and their boundaries since 260 Ma from Central America to South-eastern Asia, *Geodin. Acta 7 (4),* 169– 218, 1994.

Ricou L.E., The plate tectonic history of the past Tethys ocean, in *The ocean basins and margins, Vol. 8, The Tethys Ocean*, edited by A.E.M. Nairn, L.E. Ricou, B. Vrielynck, and J. Dercourt, pp. 3-70, Plenum Press, New York and London, 1996.

Royden, L.H., Burchfiel, B.C. and van der Hilst, R.D, The Geological Evolution of the Tibetan Plateau, *Science,* 1054-1058*,* doi:10.1126/science.1155371, 2008.

Royer, J. Y., and Patriat, P., L'Inde part à la dérive, in *Himalaya-Tibet, Le Choc des Continents*, edited by C. J. Allegre, J.-P. Avouac, and P. De Wever, pp. 25– 31, Mus. Natl. d'Hist. Nat., Paris., 2002.

Rudkevich, M. Ya., The history and the dynamics of the development of the west siberian platform, *Tectonophysics, 36 (1-3)*, 275-287, 1976.

Seward, D., Pérez-Estaún, A., and Puckov, V., Preliminary fission-track results from the southern Urals – Sterlitamak to Magnitogorsk*, Tectonophysics, 276 (1-4)*, 281-290, 1997.

Si, J., and Van der Voo, R., Too-low magnetic inclinations in central Asia: an indication of a long-term Tertiary non-dipole field?, *Terra Nova, 13*, 471-478, 2001.

Sokolov, S. Yu., Tectonic elements of the Arctic region inferred from small-scale geophysical fields, *Geotectonics, 43*, 1, 18-33, doi: 10.1134/S0016852109010026, 2009.

Sun, Z.M., Yang, Z.Y., Pei, J.L., Yang, T.S., and Wang, X.S., New Early Cretaceous paleomagnetic data from volcanic and red beds of the eastern Qaidam Block and its implications for tectonics of Central Asia, *Earth Planet. Sci. Lett., 243*, 268-281, doi:10.1016/j.epsl.2005.12.016, 2006.

Sun, Z.M., Jiang, W., Li, H.B., Pei, J.L., and Zhu, Z.M., New paleomagnetic results of Paleocene volcanic rocks from the Lhasa block: Tectonic implications for the collision of India and Asia, *Tectonophysics, 490*, 257-266, 2010.

Sun, Z.M., Pei, J.L., Li, H.B., Xu, W., Jiang, W, Zhu, Z.M, Wang, X.S., and Yang, Z.Y., Palaeomagnetism of late Cretaceous sediments from southern Tibet: Evidence for the consistent palaeolatitudes of the southern margin of Eurasia prior to the collision with India, *Gondwana Res., 21*, 53-63, 2012.

Tan, X., and Kodama, K.P., An analytical solution for correcting paleomagnetic inclination error, *Geophys. J. Int., 152*, 228-236, 2003.

Tan, X., Kodama, K.P., Chen, H., Fang, D., Sun, D., and Li, Y., Paleomagnetism and magnetic anisotropy of Cretaceous red beds from the Tarim basin, northwest China: Evidence for a rock magnetic cause of anomalously shallow paleomagnetic inclinations from Central Asia, *J. Geophys. Res., 108*, No. B2, 2107, 2003.

Tan, X., Gilder, S., Kodama, K.P., Jiang, W., Zhang, H., Xu, H., and Zhou, D, New paleomagnetic results from the Lhasa block: Revised estimation of latitude shortening across Tibet and implications for dating the India-Asia collision, *Earth Planet. Sci. Lett., 293*, 396-404, 2010.

Tapponnier, P. and Molnar, P., Active faulting and cenozoic tectonics of Tien Shan, Mongolia, and Baykal regions, *J. Geophys. Res., 84,* 3425-3459, 1979.

Tapponnier, P., Peltzer, G., Le Dain, A.Y., Armijo, R., and Cobbold, P., Propagating extrusion tectonics in Asia: New insights from simple experiments with plasticine, *Geology, 10*, 611-616, doi: 10.1130/0091-7613, 1982.

Tapponnier, P., Peltzer, G. and Armijo, R., On the mechanics of the collision between India and Asia, *Geol. Soc. Spec. Publ., 19,* 115-157, 1986.

Tauxe, L., Inclination flattening and the geocentric axial dipole hypothesis, *Earth Planet. Sci. Lett., 233*, 247-261, 2005.

Tauxe, L., and D. V. Kent, A simplified statistical model for the geomagnetic field and the detection of shallow bias in paleomagnetic inclinations: Was the ancient magnetic field dipolar?, in *Timescales of the Paleomagnetic Field*, edited by J. E. T. Channell, et al., *Geophysical Monograph, 145*, 101 – 116, 2004.

Thomas, J.-C., Chauvin, A., Gapais, D., Bazhenov, M.L., Perroud, H., Cobbold, P.R., and Burtman, V.S., Paleo-magnetic evidence for Cenozoic block rotations in the Tadjik depression (Central Asia), *J. Geophys. Res., 99*, 15,141-15,160, 1994

Torsvik, T.H., and Van der Voo, R., Defining Gondwana and Pangea palaeogeography: estimates of Phanerozoic non-dipole (octupole) fields, *Geophys. J. Int., 151*, 771-794, 2002.

Torsvik, T.H., Müller, R.D., Van der Voo, R., Steinberger, B. and Gaina, C., Global Plate Motion Frames: Toward a unified model. *Rev. Geophys., 46*, RG3004, doi:10.1029/2007RG000227, 2008.

van Hinsbergen, D.J.J., Straathof, G.B., Kuiper, K.F., Cunningham, W.D., Wijbrans, J., No vertical axis rotations during Neogene transpressional orogeny in the NE Gobi Altai: Coinciding Mongolian and Eurasian early Cretaceous apparent polar wander paths, *Geophys. J. Int., 175*, 105-128, 2008.

van Hinsbergen, D.J.J., Lippert, P.C., Dupont-Nivet, G., McQuarrie, N., Doubrovine P.V., Spakman, W., and Torsvik, T.H., Greater India Basin hypothesis and a two-stage Cenozoic collision between India and Asia, *Proc. Nat. Acad. Sci., 109*, 20, 7659-7664, 2012.

Verzhbitskii, V.E., and Kopp, M.L., Intraplate deformations in the southeastern part of the East European craton and the northeastern Indian ocean: Comparative analysis of the morphology and formation conditions, *Doklady Earth Sciences, 398*, 7, 899-903, 2004.

Verzhbitskii, V.E., and Kopp, M.L., Recent strain field of the Southern Transural region, *Doklady Earth Sciences, 405*, 8, 1170-1174, 2005.

Westphal, M., Did a large departure from the geocentric axial dipole occur during the Eocene? Evidence from the magnetic polar wander path of Eurasia, *Earth Planet. Sci. Lett., 117*, 15- 28, 1993.

Wirth, K.R, Grandy, J., Kelley, K., and Sadofsky, S., Evolution of crust and mantle beneath the Bering Sea region: Evidence from xenoliths and late Cenozoic basalts, *in* Miller, E.L., Grantz, A., and Klemperer, S.L., *eds.*, Tectonic Evolution of the Bering Shelf – Chukcha Sea – Arctic Margin and Adjacent Landmasses, *Geol. Soc. Amer. Spec. Pub., 360*, 167-193, 2002.

Yan, M., Van der Voo, R., Fang, X.M., Parés, J.M., and Rea, D.K., Paleomagnetic evidence for a mid-Miocene clockwise rotation of about 25° of the Guide Basin area in NE Tibet., *Earth Planet. Sci. Lett., 241*, 234-247, 2006.

Yang, Z., and Besse, J., Paleomagnetic study of Permian and Mesozoic sedimentary rocks from Northern Thailand supports the extrusion model for Indochina, *Earth Planet. Sci. Letters, 117*, 525-552, 1993.

Yang, Z., Courtillot,V., Besse, J., Ma, X., Xing, L., and Zhang, J., Jurassic paleomagnetic constraints on the collision of the north and South China blocks, *Geophys. Res. Lett., 19,* 577–580, 1992.

Yang, Z., Besse, J., Sutheetorn, V., Bassoulet, J.P., Fontaine, H. and Buffetaut, E., Lower-Middle Jurassic paleomagnetic data from the Mae Sot area (Thailand) : Paleogeographic evolution and deformation history of Southeastern Asia, *Earth Planet. Sci. Lett., 136,* 325-341, 1995.

Yi, Z., Huang, B., Chen, J., Chen, L., and Wang, H., Paleomagnetism of early Paleogene marine sediments in southern Tibet, China: Implications to onset of the India-Asia collision and size of Greater India, *Earth Planet. Sci. Lett., 309*, 153-165, 2011.

Zhao, X. and Coe, R.S., Paleomagnetic constraints on the collision and rotation of North and South China, *Nature, 327,* 141–144, 1987.

Figure captions.

Figure 1: (a) Orthographic projection centered on 110°E/30°N showing the location of 0 to 170 Ma selected paleomagnetic sites in Asia. Black (white) stars: localities of sampled igneous (sedimentary) rocks which have provided 159 (374) published paleomagnetic poles; Inset: abbreviations of blocks and terranes defined in the present study: AMU: Amuria, IND: India, JAP: Japan (not shown in inset), JUN: Jungar, KAZ: Kazakhstan, KH: Khorat Plateau, KOR: Korea Peninsula, KUN: Kunlun, LH: Lhasa, MB: Malaysia-Burma, MEA: Middle East Asia NCB: North China, QA: Qaidam, QI: Qiangtang, SCB: South China, SIB: Siberia, ST: Simao Terrane, TAR: Tarim; (b) and (c) geological time (in Ma) distribution of paleopoles selected in the present study by 20 Myr windows, splitted into igneous (b) and sedimentary (c) rocks results; dark (light) grey histograms: without (with) data from India; J, K, P and N stand for Jurassic, Cretaceous, Paleogene and Neogene respectively.

Figure 2: Definition of the paleolatitude anomaly ($\Delta\lambda$); this anomaly is the difference between the observed paleolatitude, as obtained from a paleomagnetic study which results in the definition of a paleopole of a given age, and the paleolatitude expected at that locality from a reference Apparent Polar Wandering Path (APWP).

Figure 3: Paleolatitude anomaly ($\Delta\lambda$) maps, contoured by 2.5° steps, as computed from selected igneous and sedimentary rocks data, using the Europe APWP (Besse and Courtillot, 2002) as a reference; (a) for 140-50 Ma period (240 data); (b) for 50-0 Ma period (182 data); hot (cold) colors underline negative (positive) anomalies; bold black line: zero $\Delta\lambda$ anomaly line; black crosses define the smoothing grid used for computation of maps (see text).

Figure 4: Paleolatitude anomaly ($\Delta\lambda$, computed as: $\Delta\lambda$ = observed λ - expected λ, in degrees) as a function of age for the Amuria block (a) and the Siberia craton (b), using the *Besse and Courtillot (2002)* APWP for Europe as a reference; bold 0 (zero) line is where the data should lie if the observed paleolatitude fits the expected one; (1), (2) and (3) time domains bounded by hatched grey lines in (a): see text; grey strips qualitatively highlight the differences between expected and observed paleolatitudes. Closed (open) symbols: data derived from igneous (sedimentary) rocks; dark grey areas in stereoplots indicate the

blocks/terranes relevant to displayed data; n is the number of data from each block/terrane.

Figure 5: Paleolatitude anomaly (Δλ) as a function of age for North China and Korea blocks/terranes (a) and South China Block (b) , using *Besse and Courtillot (2002)* APWP for Europe as a reference; same conventions as in Fig. 4.

Figure 6: A new reference APWP for East Asia based on paleopoles obtained from: (a) 66 igneous (black stars) and 80 sedimentary (white stars) rocks collected from localities (dark grey areas in the projection) of Siberia (SIB), Amuria (AMU), Korea (KOR), North and South China blocks (NCB and SCB); circled white star: reference point *(R)* at {45°N, 120°E} used to compute the angular difference quoted in (f); (b), (c), (d): Three examples of East Asia APWP mean poles at 20 Ma (b), 50 Ma (c) and 100 Ma (d), computed as a mixed average between fixed paleopoles (circles) and small-circles (dotted lines) passing through the rotated paleopoles (squares) and centered on sites location (stars); black (white) symbols: paleopoles from igneous (sedimentary) formations; large white star with A_{95} circle of confidence: mixed average between fixed points and small-circles passing through the rotated paleopoles (see text); bold black lines: best-fit small-circles (Mardia and Gadsden, 1977) over the paleopoles, centered on sites location, with 95% confidence areas (grey strips); (e) and (f): white dots: Besse and Courtillot (2002) APWP for Europe; black dots: new East Asia APWP with (e) and without (f) their circles of 95% confidence; paleopole ages in Ma are given in (f); grey sectors in (e) and (f): azimuth of localities viewed from the north pole; grey strips with curved lines in (f) are the small-circles computed on the 10-60 Ma poles from the Europe APWP (Besse and Courtillot, 2002) and the present APWP for East Asia, centered on the arbitrary reference point at {45°N, 120°E} (white star) . (a): orthographic projection, (b), (c) and (d): orthographic projections of the north hemisphere, (e) and (f): equal-area projections centered on the north pole, and limited to the 70°N latitude.

Figure 7: Checking East Asia APWP - 1: Paleolatitude anomaly (Δλ) of sedimentary (a) and igneous (b) rocks from localities in Siberia and eastern Chinese and Korean blocks as a function of age, using the East Asia APWP as a reference; dotted lines with grey areas: average Δλ discrepancies with 2σ variances between the observed and the expected paleolatitudes, computed by 50 Myrs age windows, as displayed in insets; same conventions as in Figure 4.

Figure 8: Checking East Asia APWP - 2: Paleolatitude anomaly (Δλ) of sedimentary and igneous rocks from the Japan islands as a function of age, using the Europe (a) and the East Asia (b) APWP as a reference; dotted line with grey area: average Δλ discrepancy with 2σ variance between the observed and the expected paleolatitudes, as displayed in inset; same conventions as in Figure 4.

Figure 9: Paleolatitude anomaly (Δλ) maps of Asia, contoured by 2.5° steps, as constructed from selected effusive and sedimentary rocks data, using the East Asia APWP as a reference; (a) for the 140-50 Ma period (240 data); (b) for the 50-0 Ma period (182 data); hot (cold) colors underline negative (positive) anomalies; black crosses define the smoothing grid used for computation of the maps (see text). These maps are to be compared to the maps of Fig. 3.

Figure 10: Paleolatitude anomaly (Δλ) as a function of age for (a) the Tibetan and (b) the Indochina blocks, using the present study APWP for East Asia (defined in section §4 and Fig. 6) as a reference; symbols are: (a) circles, squares and triangles for the Lhasa, Qiangtang and Kunlun blocks respectively; (b) triangles, circles and squares for the Simao terrane, the Khorat plateau and Malaysia-Burma respectively; (a) the average discrepancies are drawn as bold lines, with their 95% areas of confidence (grey areas), for all Tibetan blocks (a) and Indochina blocks (b), and in dotted bold line for the Lhasa block only in (a); mention (1) (resp. (2)): amount of divergence between the Lhasa block and the Indochina peninsula after 140-50 Ma (resp. 0-50 ma) data; large dashed vertical grey lines underline the 50 Ma limit we have imposed in our analysis; open/closed symbols and other conventions: same as in Fig. 4.

Figure 11: Paleolatitude anomaly (Δλ) as a function of age for (a) the Qaidam block, and (b) the Tarim (circles) and Jungar (squares) blocks, using the present study APWP for East Asia (defined in section §4 and Fig. 6) as a reference; open/closed symbols and other conventions: same as in Fig. 10.

Figure 12: (a) Paleolatitude vs. time evolution of a reference point currently situated at {29°N, 86°E} (grey stars) (1) predicted from the APWPs of Besse and Courtillot (2002) for Europe (blue curve, with dark grey 95% confidence area); (2) from our new East Asia APWP (red curve, with light grey 95% confidence area); (3) from the APWP of Besse and Courtillot (2002) for India (black curve with blue 95% confidence area); dotted black

curve (4): inferred paleolatitude evolution of the northern edge of a 10° wide Greater India at the longitude of our reference point, after Besse et al. (1984); (5) inferred Lhasa block paleolatitudinal evolution (red dotted curve, with light grey 95% confidence area); (b) 80 to 20 Ma and -10° to 35°N enlargment as circled in (a); red star: Lhasa and Greater India curves crossing, our proposed time and place of the India collision with Eurasia; yellow stars labelled (1) to (9) are latitudes and ages of India Eurasia collision derived from: (1) Aitchison et al. (2007), (2) Tan et al. (2010), (3) Dupont-Nivet et al. (2010a), (4) Sun et al. (2012), (5) Liebke et al. (2010), (6) Sun et al. (2010), (7) Chen et al. (2010), (8) Patzelt et al. (1996) and (9) Yi et al. (2011).

Figure 13: Cenozoic (0 - 50 Ma) paleolatitude anomaly (Δλ) maps, contoured by 2.5° steps, of Asia as constructed from selected effusive and sedimentary rocks data, using the BC02 Europe APWP as a reference, but taking into account non-dipolar quadrupolar (G2) and octupolar (G3) field components; 2 models are illustrated following the suggestions of *Si and Van der Voo (2001)*: (a) g_2^0 = 0% and g_3^0 = 10% (G2 = 0.00; G3 = 0.10); (b) g_2^0 = 0% and g_3^0 = 15% (G2 = 0.00; G3 = 0.15); see text.

Figure 14 (a-b): Orthographic projections, constructed with *PaleoMac* (Cogné, 2003), of schematic paleogeographic reconstructions of the Eurasia plate between 90 Ma (a) and Present (f), based on a purely tectonic interpretation of the paleomagnetic shallow-inclinations, or low-latitudes anomaly in Asia, in the hypothesis of a dipolar magnetic field. Dark orange areas are the present-day continental contours, light orange/yellow areas are continental shelves and/or intracontinental shortened and/or consumed continental segments (including Greater India); bold black continental contour with white background in (b) to (e): paleoposition of east Eurasia as deduced from the BC02 reference APWP for Europe; bold lines with triangles: main subduction (blue) or thrust (red) zones; black plain or dotted lines: tectonic limits; all arrows indicate relative movements, as observed in the field, see references in text; red large arrows: converging and diverging relative movements across tectonic limits; black arrows: shear sense along transform and/or strike-slip limits; question marks indicate hypothesized movements, limits, and/or paleopositions of terranes; grey sector with white arrows in (b): see text; red normal fault symbols in (e) and (f), along MOS, schematize WNW-ESE Oligocene to Present opening of the major Lake Baikal Rift (e.g. Petit and Deverchère, 2006); abbreviations in all stereoplots (a) to (f) are for: AR: Alpha Ridge, GR: Gakkel Ridge, JS:

Japan Sea, KR: Knippovich Ridge, MOS: Mongol-Okhotsk Suture, RR: Run Ridge, TTL: Tornquist-Tesseyre Line, UM: Ural Mountains.

Figure 14 (c-d) - *continued* .

Figure 14 (e-f) - *continued*.

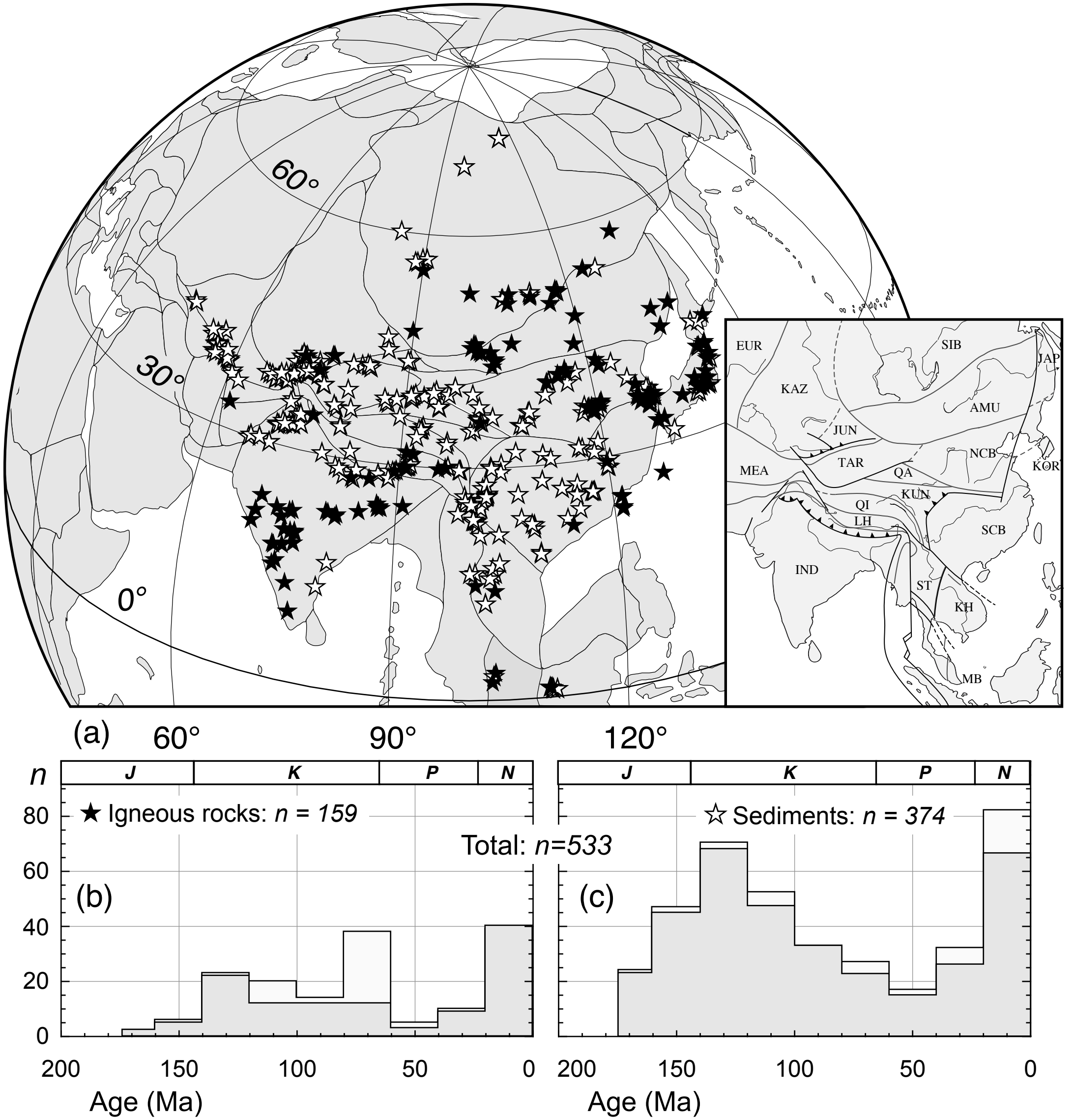
60°
30°
0°
60°
90°
120°
(a)
EUR
SIB
JAP
KAZ
AMU
JUN
NCB
KOR
TAR
QA
MEA
KUN
QI
LH
SCB
IND
ST
KH
MB
n
J
K
P
N
★ Igneous rocks: n = 159
☆ Sediments: n = 374
Total: n=533
(b)
(c)
80
60
40
20
0
200
150
100
50
0
Age (Ma)

Figure 1

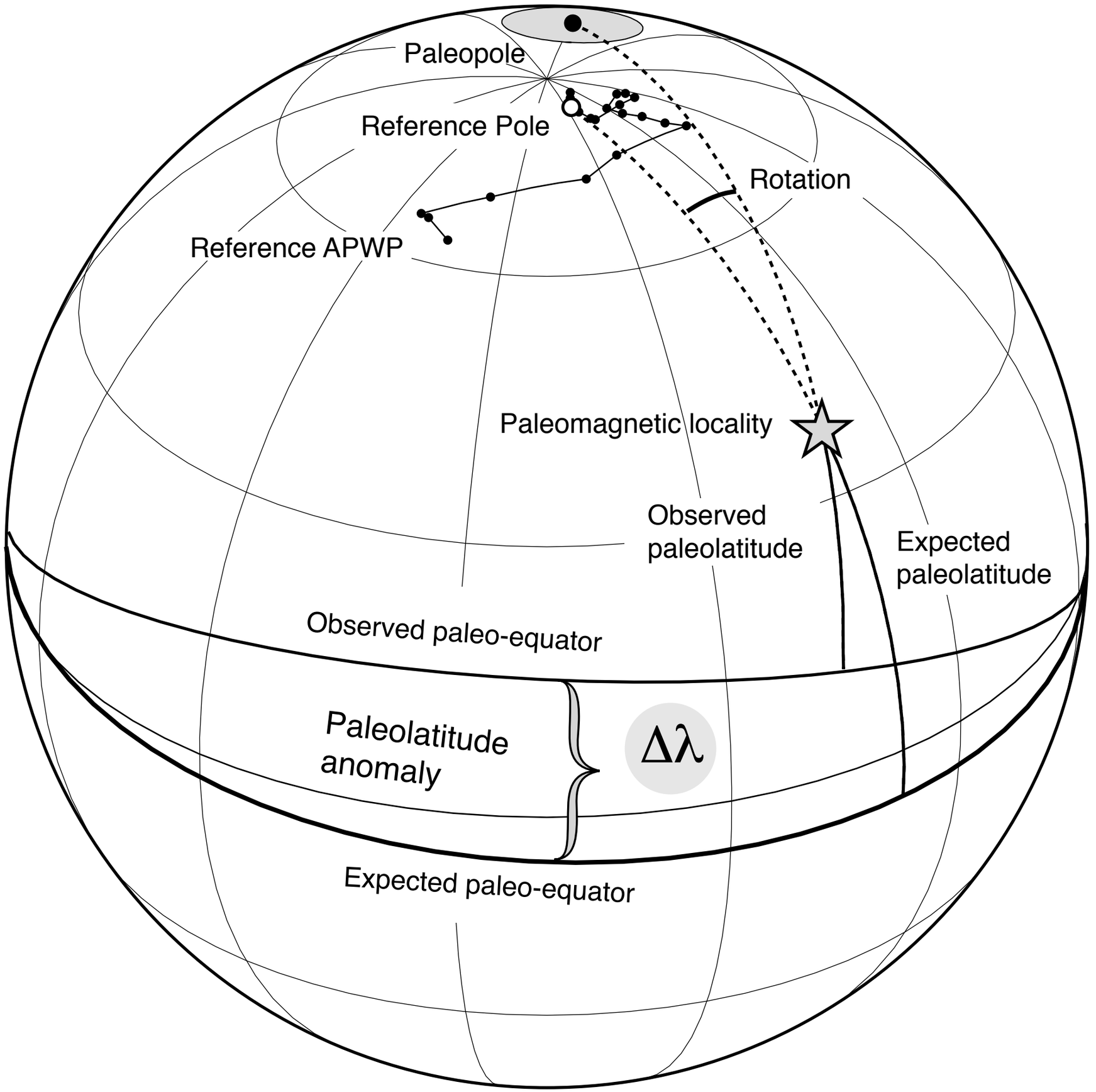
Paleopole
Reference Pole
Rotation
Reference APWP
Paleomagnetic locality
Observed
paleolatitude
Expected
paleolatitude
Observed paleo-equator
Paleolatitude
anomaly
Δλ
Expected paleo-equator

Figure 2

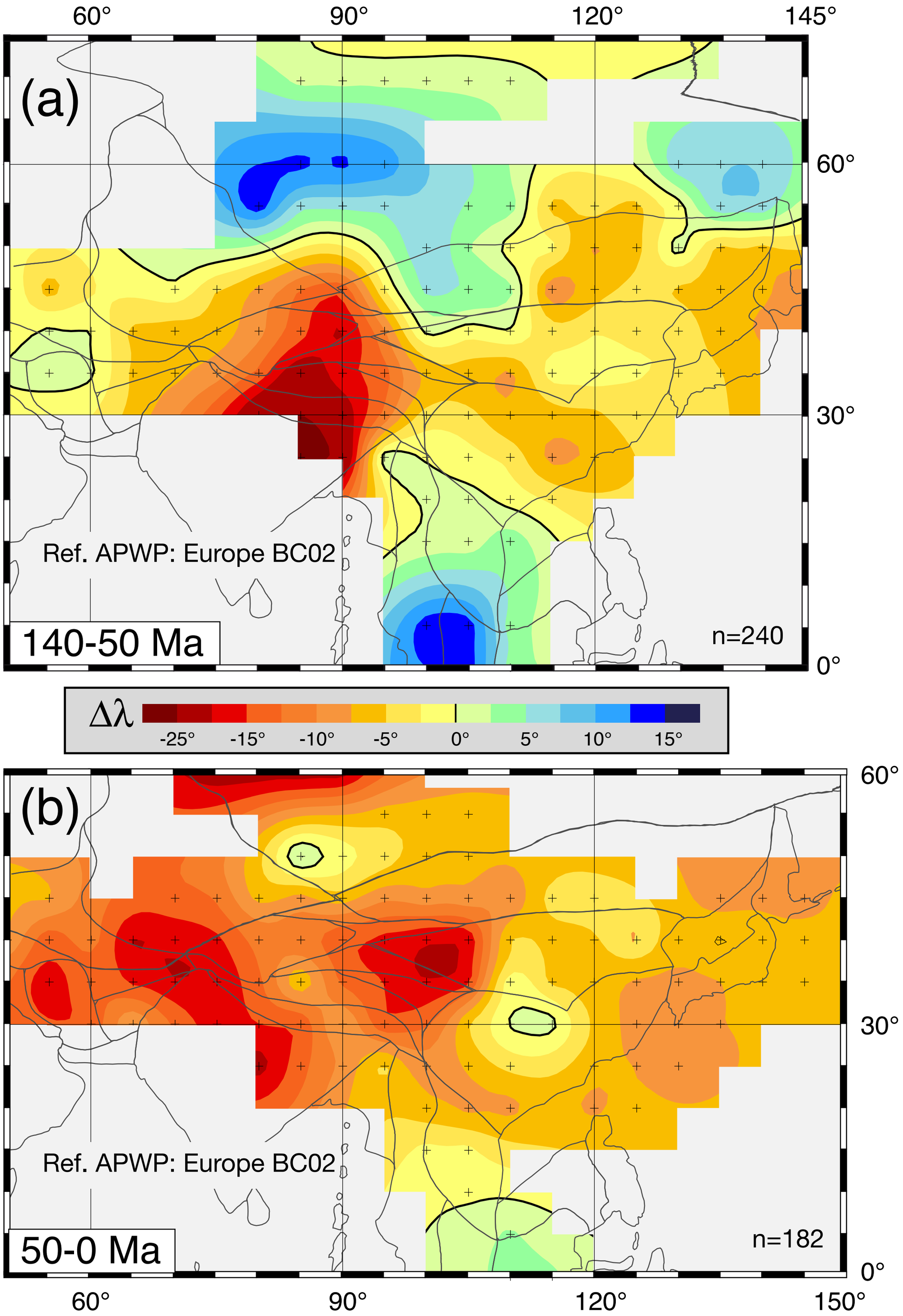
60°
90°
120°
145°
(a)
60°
30°
0°
Ref. APWP: Europe BC02
140-50 Ma
n=240
Δλ
-25°
-15°
-10°
-5°
0°
5°
10°
15°
(b)
60°
30°
0°
Ref. APWP: Europe BC02
50-0 Ma
n=182
60°
90°
120°
150°

Figure 3

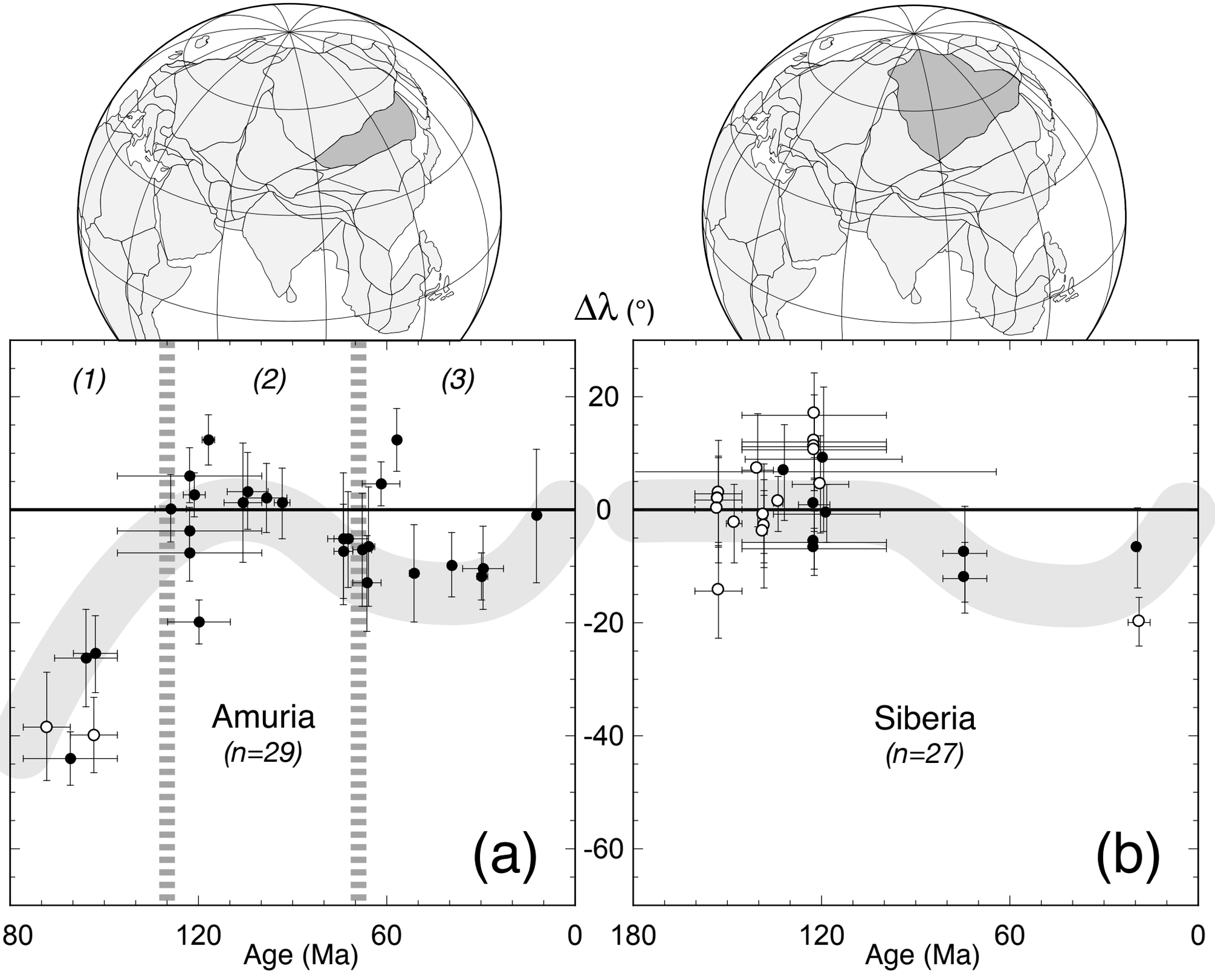

Figure 4

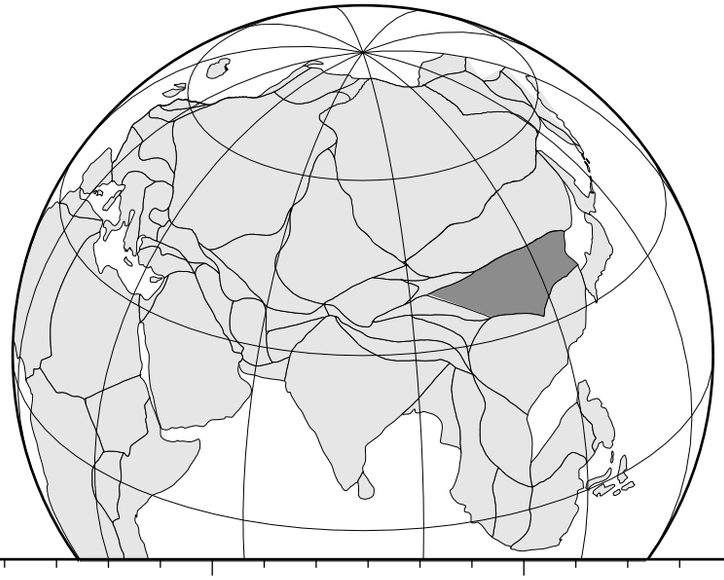

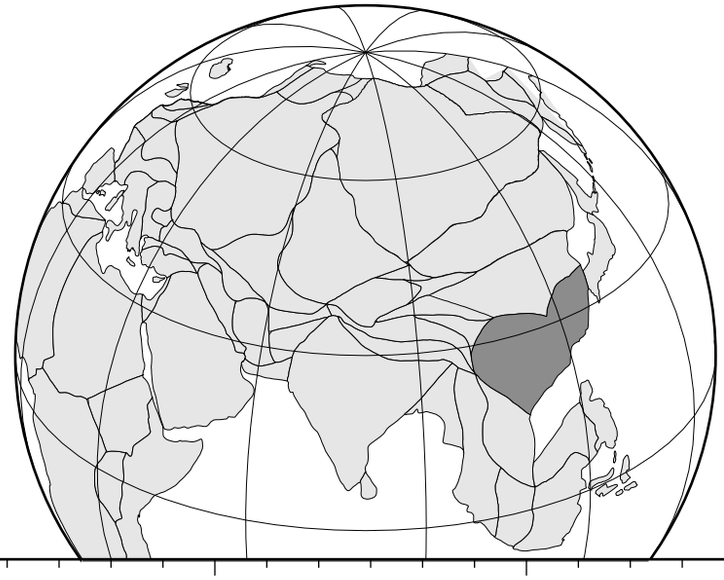

$\Delta\lambda$ (°)

20

0

-20

-40

-60

NCB+KOR
(n=64)

(a)

SCB
(n=60)

(b)

180 120 60 0
Age (Ma)

180 120 60 0
Age (Ma)

Figure 5

SIB
AMU
KOR
NCB
SCB
★ igneous rocks n = 66
☆ sediments n = 80
(a)
(b)
(c)
(d)
(e)
(f)
180
270
90
0
70°N
20 Ma
50 Ma
100 Ma
140
150
130
120
160
110
90
80
70
50
100
70
100-130
60
20
40
30
10
0
(R)
9.2° ± 1.8°
(10 - 60 Ma)

Figure 6

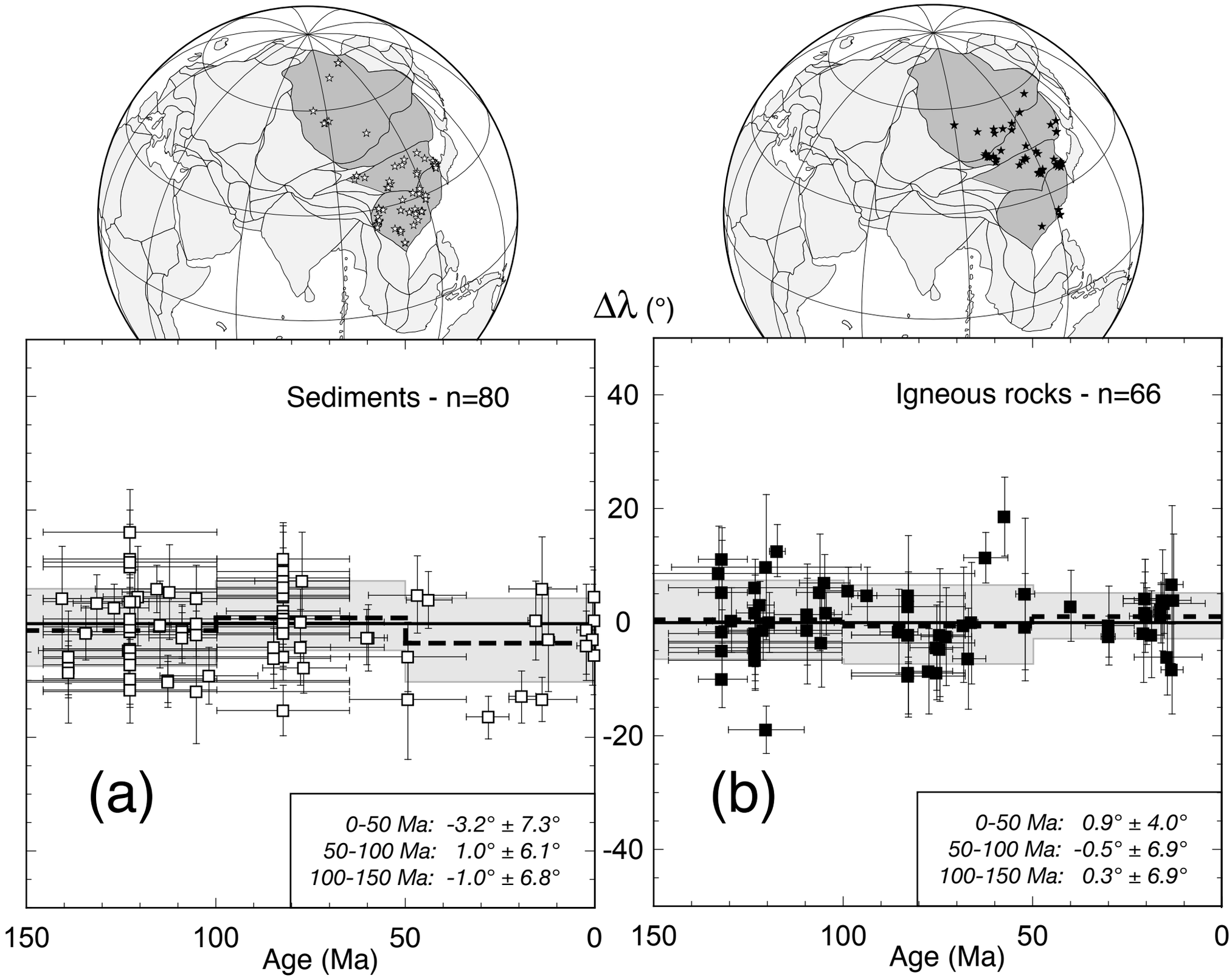
Δλ (°)
Sediments - n=80
Igneous rocks - n=66
40
20
0
-20
-40
(a)
(b)
0-50 Ma: -3.2° ± 7.3°
50-100 Ma: 1.0° ± 6.1°
100-150 Ma: -1.0° ± 6.8°
0-50 Ma: 0.9° ± 4.0°
50-100 Ma: -0.5° ± 6.9°
100-150 Ma: 0.3° ± 6.9°
150
100
50
0
Age (Ma)

Figure 7

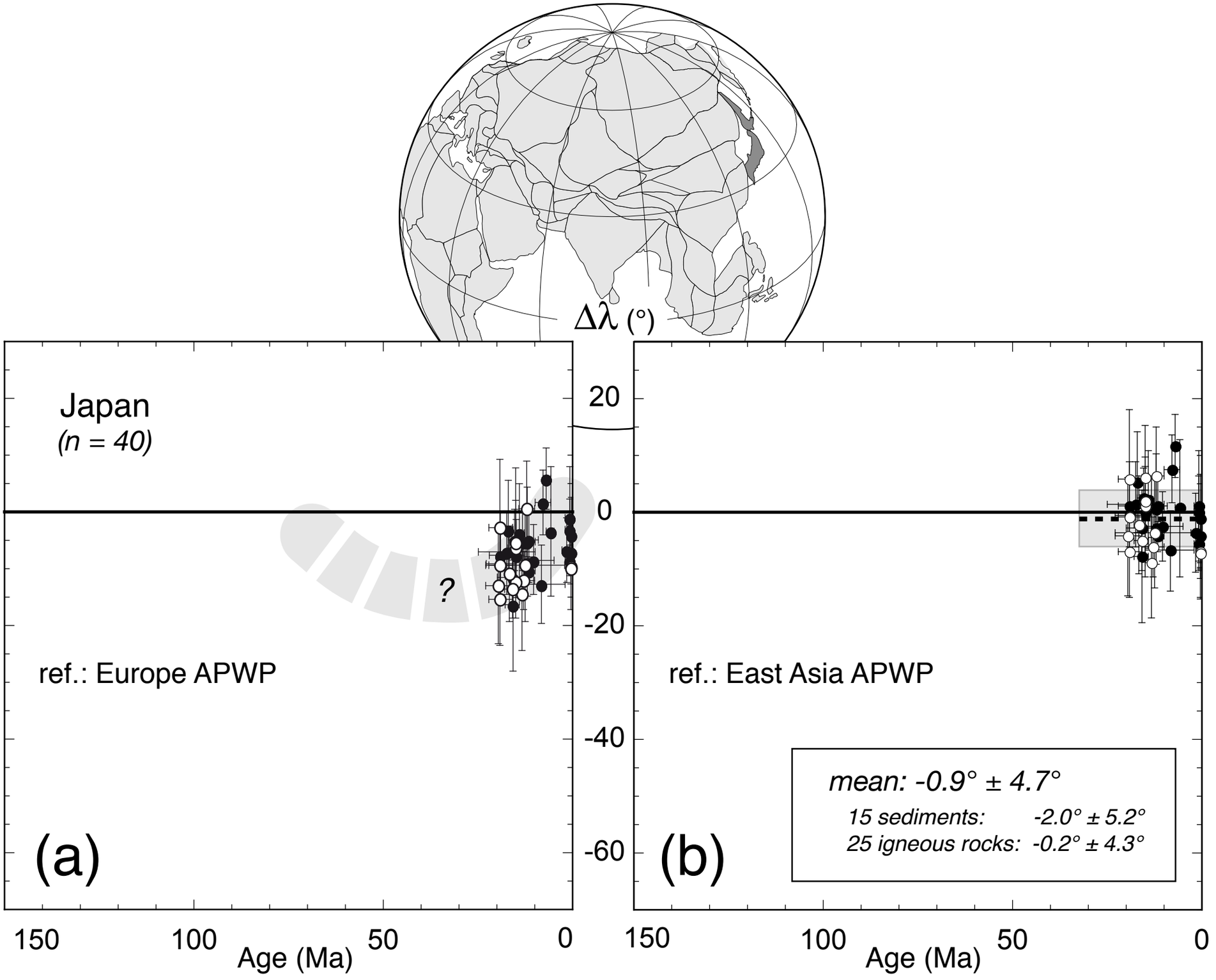
Δλ (°)
Japan
(n = 40)
?
ref.: Europe APWP
ref.: East Asia APWP
mean: -0.9° ± 4.7°
15 sediments: -2.0° ± 5.2°
25 igneous rocks: -0.2° ± 4.3°
(a)
(b)
20
0
-20
-40
-60
150
100
50
0
Age (Ma)

Figure 8

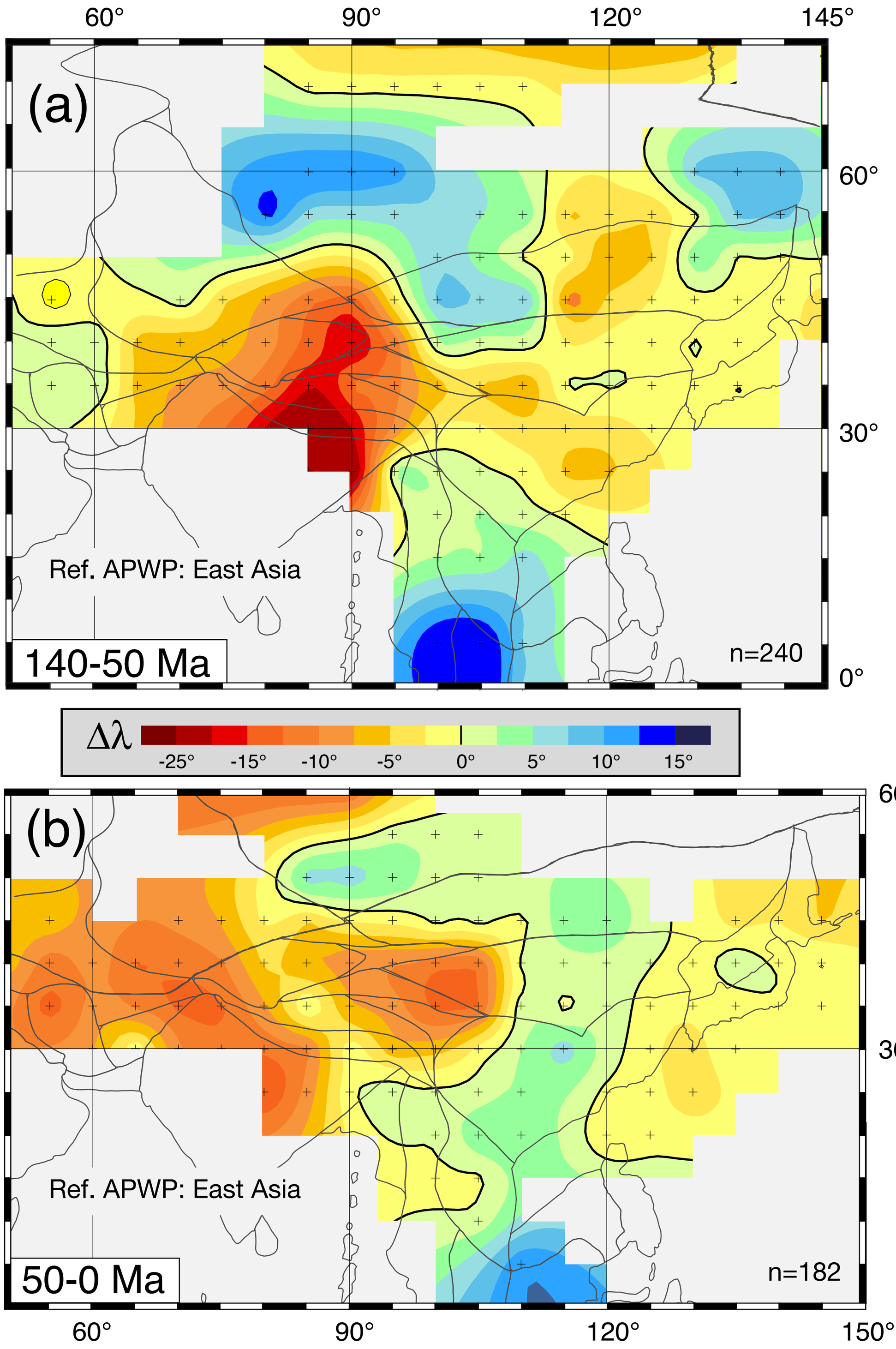
60°
90°
120°
145°
(a)
60°
30°
0°
Ref. APWP: East Asia
140-50 Ma
n=240
Δλ
-25°
-15°
-10°
-5°
0°
5°
10°
15°
(b)
60°
30°
Ref. APWP: East Asia
50-0 Ma
n=182
60°
90°
120°
150°

Figure 9

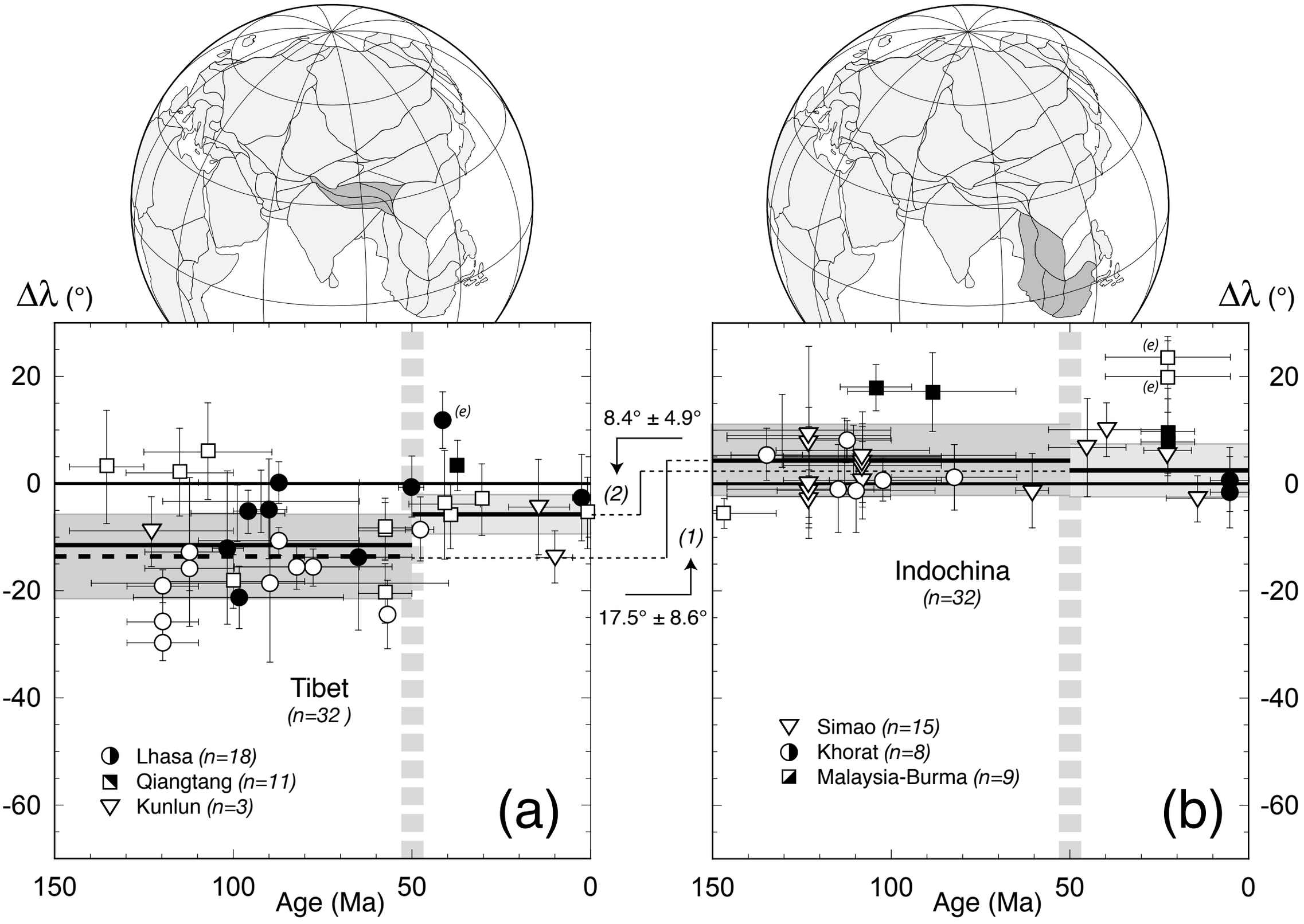

Mean Δλ *(using East Asia APWP as a reference)*:

- - Lhasa block	- 140 - 50 Ma:	Δλ = -13.2° ± 8.5°, n = 19
— Tibet all	- 140 - 50 Ma:	Δλ = -11.3° ± 9.2°, n = 27
	- 50 - 0 Ma:	Δλ = -6.0° ± 3.6°, n = 8

Mean Δλ *(using East Asia APWP as a reference)*:

- INC peninsula	- 140 - 50 Ma:	Δλ = + 4.3° ± 6.6°, n = 22
	- 50 - 0 Ma:	Δλ = + 2.4° ± 5.0°, n = 10

Figure 10

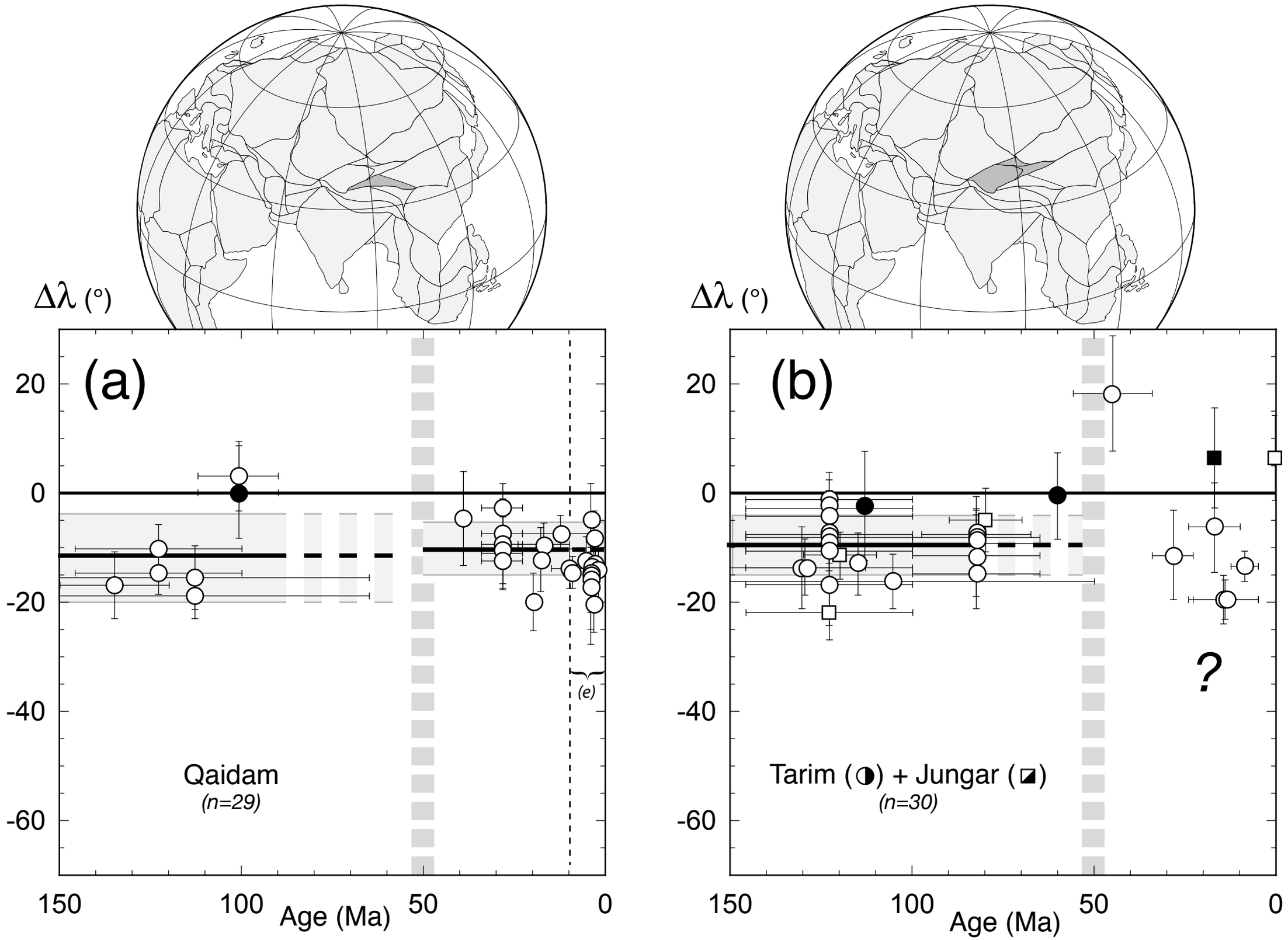

Mean Δλ *(using East Asia APWP as a reference)*:
- 140 - 50 Ma: Δλ = -11.9° ± 8.0°, n = 6
- 50 - 10 Ma: Δλ = -10.3° ± 4.5°, n = 13

Mean Δλ *(using East Asia APWP as a reference)*:
- 140 - 50 Ma: Δλ = -9.7° ± 5.5°, n = 22
- 50 - 0 Ma: *scattered (-20° to +20°)*

Figure 11

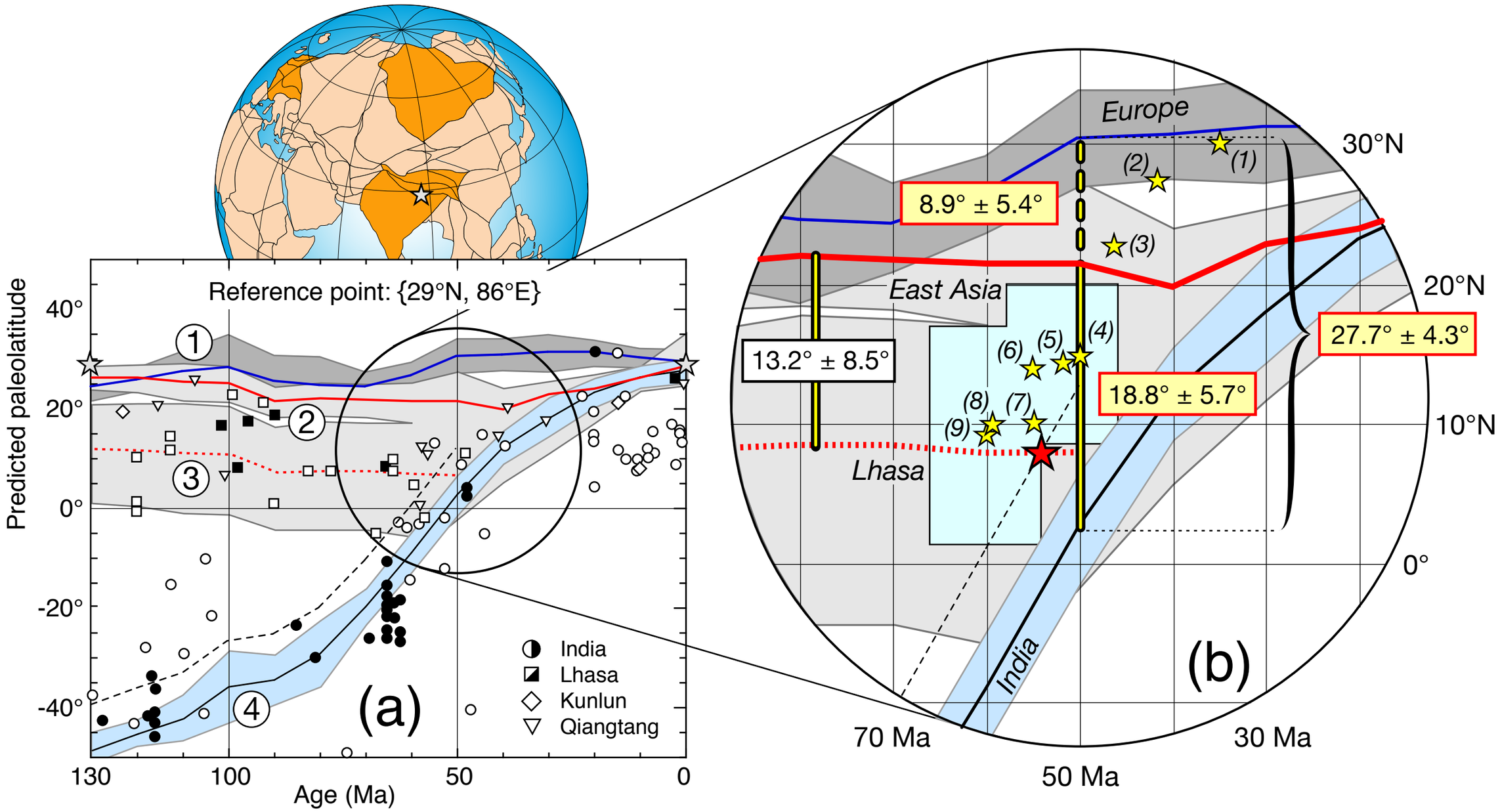
Reference point: {29°N, 86°E}
Predicted paleolatitude
40°
20°
0°
-20°
-40°
130
100
50
0
Age (Ma)
①
②
③
④
(a)
India
Lhasa
Kunlun
Qiangtang
Europe
East Asia
Lhasa
India
(1)
(2)
(3)
(4)
(5)
(6)
(7)
(8)
(9)
8.9° ± 5.4°
13.2° ± 8.5°
18.8° ± 5.7°
27.7° ± 4.3°
30°N
20°N
10°N
0°
70 Ma
50 Ma
30 Ma
(b)

Figure 12

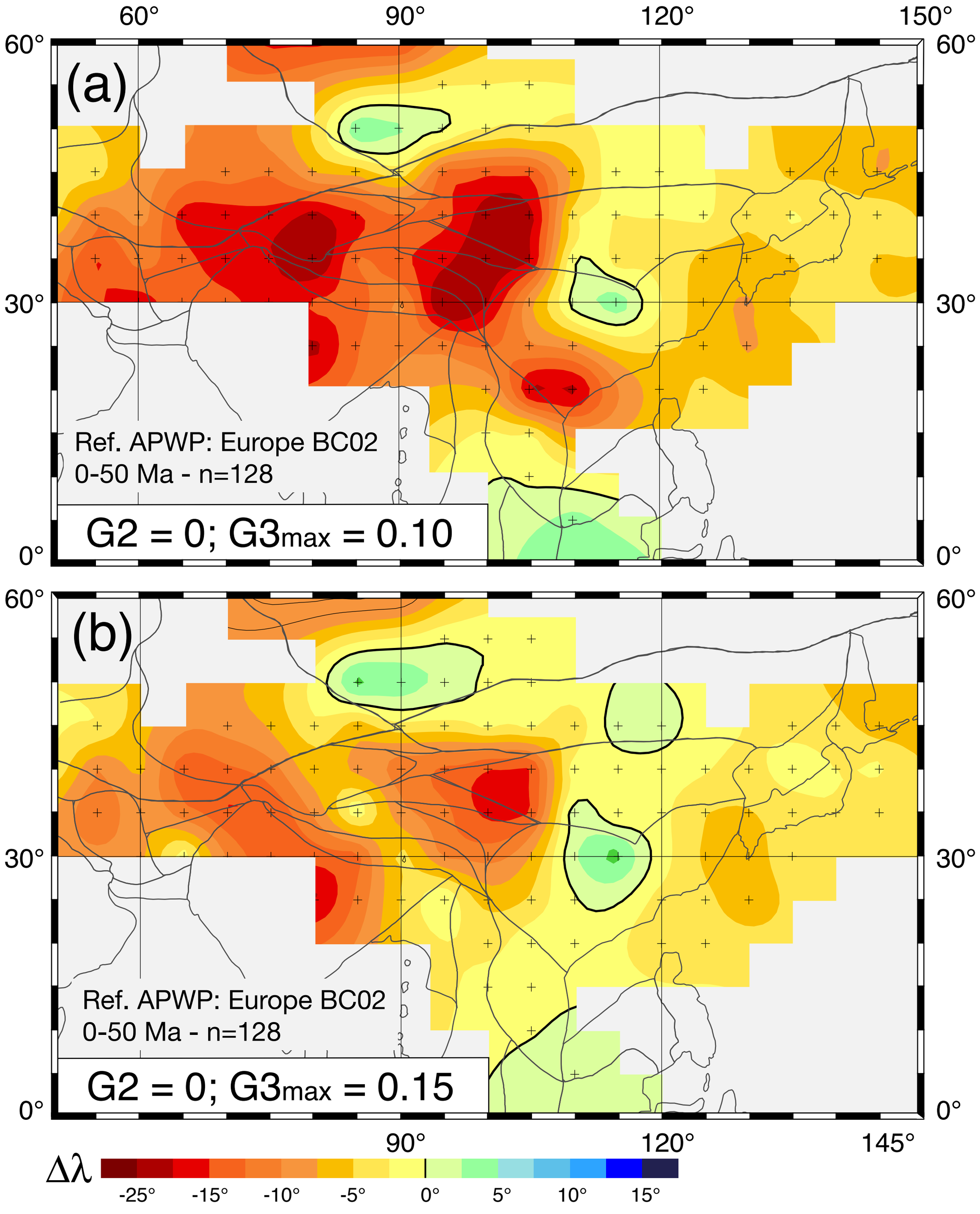
60°
90°
120°
150°
60°
30°
0°
(a)
Ref. APWP: Europe BC02
0-50 Ma - n=128
G2 = 0; G3max = 0.10
(b)
Ref. APWP: Europe BC02
0-50 Ma - n=128
G2 = 0; G3max = 0.15
90°
120°
145°
Δλ
-25°
-15°
-10°
-5°
0°
5°
10°
15°

Figure 13